Very-high resolution aerial imagery and deep learning uncover the fine-scale spatial patterns of elevational treelines

Erik Carrieri[1], Donato Morresi[1], Fabio Meloni[1], Nicolò Anselmetto[1], Emanuele Lingua[2], Raffaella Marzano[1], Carlo Urbinati[3], Alessandro Vitali[3], Matteo Garbarino[1]

[1]Department of Agricultural, Forest and Food Sciences, University of Turin, Grugliasco, 10095, Italy
[2]Dept. of Land, Environment, Agriculture, University of Padova, Legnaro, 35020 ,Italy
[3]Dept. of Crop, Food and Environmental Sciences, Marche Polytechnic University, Ancona, 60131, Italy

Correspondence to: Erik Carrieri (erik.carrieri@unito.it)

Abstract. Treelines are sensitive indicators of global change, as their position, composition and pattern directly respond to ecological and anthropogenic factors. However, several treeline studies remain case-specific, focusing on local patterns and processes. Treelines worldwide exhibit a great variability even within single landscapes, which limits the reliability of modeled spatial patterns, and the generalizability of findings based on case studies. Advancing methods to accurately map fine-scale treeline spatial patterns over large extents is crucial to overcome this limitation. Innovative approaches integrating remote sensing with uncrewed aerial vehicles (UAV) and deep learning offer a promising way to bridge the gap between field-based observations of fine-scale patterns and their large-scale implications, ultimately informing and supporting practices for the conservation of forest ecosystems in the face of ongoing and future ecological challenges.

In this study, we combined field data and UAV-based remote sensing with a deep learning model to retrieve individual tree-scale information across 90 ha in 10 study sites in the Italian Alps. Using the proposed methodology, we were able to correctly detect individual tree crowns of conifers taller than 50 cm with a detection rate of 70% and an F1 score of 0.76. Accuracy increased with tree height, reaching 86% for trees taller than 2 m. Canopy delineation was robust overall (Intersection over Union, IoU = 0.76) and excellent for tall trees (IoU = 0.85). Tree position and height estimates achieved RMSEs of 59 cm and 92 cm, respectively.

Both univariate and bivariate Point Pattern Analysis (PPA) revealed clustering for scales < 20 m and a strong spatial repulsion between small and tall trees across all the tested spatial scales. Our results demonstrated that the proposed methodology effectively detects, delineates, georeferences, and measures the height of most trees across diverse Alpine treeline ecotones. This enables the analysis of fine-scale spatial patterns and enhances the interpretation of underlying ecological processes. The inclusion of heterogeneous study areas facilitates the transferability of the segmentation model to other mountain regions and

offers a benchmark for developing a global network of fine-scale mapped treeline spatial patterns to monitor the effects of global change on ecotone dynamics.

1 Introduction

The elevational treeline is the transition zone from the uppermost closed montane forest (timberline) to the highest scattered trees (tree species line) (Holtmeier et al., 2003), and one of the most studied ecotones. Since the late 19th century, scientific studies largely focused on the diversity and complexity of factors affecting the ecotone spatial and temporal patterns at different scales (Hansson et al., 2021; Holtmeier, 2009). It is well known that temperature plays a crucial role in treeline positioning and dynamics from regional to global scales (Dirnböck et al., 2003; Gehrig-Fasel et al., 2007; Harsch et al., 2009; Körner & Paulsen 2004), but is not the only driving factor. Many other studies have emphasised the significant role of other factors in treeline formation (Mienna et al., 2024), including water availability (Barros et al., 2017; Williams et al., 2013), site topography (Leonelli et al., 2016; Marquis et al., 2021; Müller et al., 2016), biotic drivers (Brown and Vellend, 2014; Cairns et al., 2007) and anthropogenic pressure (Gehrig-Fasel et al., 2007; Malandra et al., 2019; Vitali et al., 2019).

Global change can trigger large-scale vegetation dynamics affecting the provision of ecosystem services - such as carbon sequestration (Hansson et al., 2021; Zierl and Bugmann, 2007). Climate alteration can induce upward migration of species, threatening a loss of habitat and biodiversity of high alpine communities (Kyriazopoulos et al., 2017). This sensitivity to climatic and anthropogenic factors makes high-elevation ecotones key indicators of global change (Dirnböck et al., 2011; Greenwood and Jump, 2014). Monitoring changes at elevational treelines is therefore of utmost importance to follow how forests are responding and to forecast how they will respond to a changing environment (Chan et al., 2024; Hansson et al., 2023; Mottl et al., 2021) and ultimately to guide the definition of appropriate conservation strategies. However, understanding vegetation changes in response to the complex interplay of these drivers requires studying highly heterogeneous systems across broad spatial and temporal gradients (Holtmeier and Broll, 2007, 2017).

An open question in many areas of ecology is how to infer processes from observed patterns. In forest ecosystems, tree spatial distributions retain critical signatures of historical dynamics and can be used to derive insights into underlying ecological processes (Grimm et al., 2005; McIntire and Fajardo, 2009; Salazar Villegas et al., 2023). For instance, tree distribution can reveal species-specific coping strategies under stressful conditions, such as the ones found in the altitudinal treeline ecotones, where positive facilitative interactions may prevail (Callaway, 1995, 1998; Smith et al., 2003). Alternatively, tree spatial patterns may reflect the result of intra- and interspecific interactions, encompassing both facilitative and competitive associations (Getzin et al., 2006; Salazar Villegas et al., 2023). Assessing these spatial association patterns among species can help to disentangle the mechanisms shaping treeline structure and dynamics. In this context, the great spatial heterogeneity observed in high-elevation ecotones provides a great opportunity to investigate pattern-process relationships. However, this same heterogeneity constrains the extrapolation of case-specific observations, thereby limiting their broader ecological generalization. How to tackle the spatial heterogeneity issue is still an open question, and consequently the attribution of the observed processes to specific drivers is still a challenge (Garbarino et al., 2023). Combining ground-based and remote sensing (RS) data could be a winning venue to solve this compelling issue, especially if pursued with a flexible and efficient protocol. Field surveys remain the traditional methods used also at treelines and involve measuring several tree parameters (e.g. stem

DBH, height, position, health conditions) within small study areas – plots or transects (Mainali et al., 2020; Van Bogaert et al., 2011; Vitali et al., 2017, 2019). This approach provides high-resolution, high-quality data applicable to a broad array of ecological investigations. However, its time-intensive nature, coupled with the limited spatial extent and discontinuous distribution of plots or transects, may reduce the representativeness of the broader landscape.

At this point, remote sensing techniques come into play. Although their application in treeline studies dates back to the 1980s (Holmgren and Thuresson, 1998), it is only over the last two decades that RS has been widely adopted in treeline ecology (Garbarino et al., 2023). The choice of the right RS tool depends on the spatial and temporal scale required to address a given research question. For instance, while satellite imagery can provide suitable data over large forest areas and long time periods (Garbarino et al., 2020; Nguyen et al., 2024), most optical sensors lack the spatial resolution necessary for individual tree mapping (Bennett et al., 2024; Morley et al., 2018; Simard et al., 2011). The limitations of field surveys (limited spatial and temporal extent) and satellite-based data (high spatial and temporal extent but low resolution) can be overcome by using Uncrewed Aerial Vehicle (UAV) platforms (Fromm et al., 2019; Qin et al., 2022; Xie et al., 2024). Their growing availability and ease of deployment make UAVs increasingly valuable for applications such as detailed tree mapping. In addition to wall-to-wall mapping of relatively large and heterogeneous areas, UAVs survey enables the analysis of fine-scale drivers and the extraction of tree attributes and features (Nasiri et al., 2021; Panagiotidis et al., 2017; Shimizu et al., 2022; Xiang et al., 2024).

Single-tree mapping approaches are crucial in treeline ecology, as they provide insights into the underlying ecological processes shaping treeline pattern and structure. Seedling establishment - a key driver of plant community dynamics - heavily depends on the presence and availability of microsites that provide suitable conditions for growth and survival (Frei et al., 2018). Multiple local factors such as topography, vegetation, and herbivory influence tree recruitment and thus mediate treeline dynamics (Elliott and Kipfmueller, 2010; Lett and Dorrepaal, 2018; Ramírez et al., 2024). Neighbouring vegetation can either hinder or enhance tree recruitment through competitive or facilitation associations (Getzin et al., 2006; Getzin et al., 2006; Salazar Villegas et al., 2023; Smith et al., 2003). Whether these interactions result in a positive or negative feedback depends on the fine-scale interplay between biotic and abiotic factors. The resulting spatial patterns at the individual tree-scale provide a valuable perspective to both infer past processes and predict future trajectories. Accurate high-resolution single-tree maps are essential tools needed to capture these fine-scale patterns and investigate such tree–tree interactions.

Convolutional Neural Networks (CNNs) combined with very-high-resolution images are a reliable and versatile tool for single-tree scale analyses, enabling the accurate identification and representation of different plant species and communities as well as the detection of individual trees (Braga et al., 2020; Fricker et al., 2019; Fromm et al., 2019; Kattenborn et al., 2021). The latter can be achieved through instance segmentation algorithms that enable the detection of individual objects on the input images, allowing to distinguish and separate individual interwoven tree canopies (Ball et al., 2023; Braga et al., 2020). Despite the widespread use of UAV for individual tree mapping and tree features detection in several forest ecosystems (Dietenberger et al., 2023; Diez et al., 2021; Weinstein et al., 2019), the distinctive species composition, stratified horizontal and vertical structure, and complex terrain characteristics of treeline ecotones confer a unique ecological identity to these environments.

Therefore, a framework for mapping fine-scale tree spatial patterns at treeline ecotones based on low-cost UAV imagery is needed.

In this regard, the present study tests the following hypotheses: (i) the integration of UAV derived very high-resolution RGB imagery with CNNs models enables accurate single-tree level detection to infer ecological processes from treeline patterns; (ii) the trained model exhibits sufficient generalizability to perform reliably on heterogeneous datasets, maintaining high accuracy in detecting individual trees, delineating crown boundaries, and estimating their position and height; and (iii) that spatial patterns derived from the fine-scale treeline maps can reveal ecologically meaningful tree-to-tree interactions, thereby supporting their application in the study of treeline dynamics and underlying ecological processes.

2 Materials and Methods

2.1 Study Area

We selected ten study sites across the Italian Alps (Fig. 1) spanning a broad longitudinal gradient representative of the Western, Central, and Eastern Italian Alps. This selection ensured a balanced dataset encompassing highly heterogeneous climatic, topographical, soil, and vegetational conditions (Appendix A). Introducing such heterogeneity allowed us to test the transferability of the protocol to several treeline conditions. The selected treelines present elevations ranging between 2100 and 2400 m a.s.l., and variable slope aspects due to the differing orientations of the valleys. Above the closed forest, soils include both mesic and xeric regions and feature patches of grasslands, sparsely vegetated areas, screes, and surfaces shaped by gravitational events such as rill and gullies. All the selected landscapes experienced centuries of human land-use practices under varying intensities of management pressure. In general, land abandonment is more marked in the Western sector of the study area (Bätzing et al., 1996). Across all sites, the mean annual temperature ranges between 0 C° and 2 C°, while the mean annual precipitation varies from 800 mm to 1800 mm. Reflecting the typical species composition of the subalpine belt in the Alps, in all the studied treelines the dominant treeline-forming species are European larch (*Larix decidua* Mill.) and Swiss stone pine (*Pinus cembra* L.). Other species present include Norway spruce (*Picea abies* (L.) H.Karst.), dwarf mountain pine (*Pinus mugo* Turra), mountain pine (*Pinus uncinata* Miller), Scots pine (*Pinus sylvestris* L.), as well as few broadleaf species such as green alder (*Alnus viridi*s (Ehrh.) K. Koch) and silver birch (*Betula pendula* Roth). Further details on the study sites are provided in Table 1.

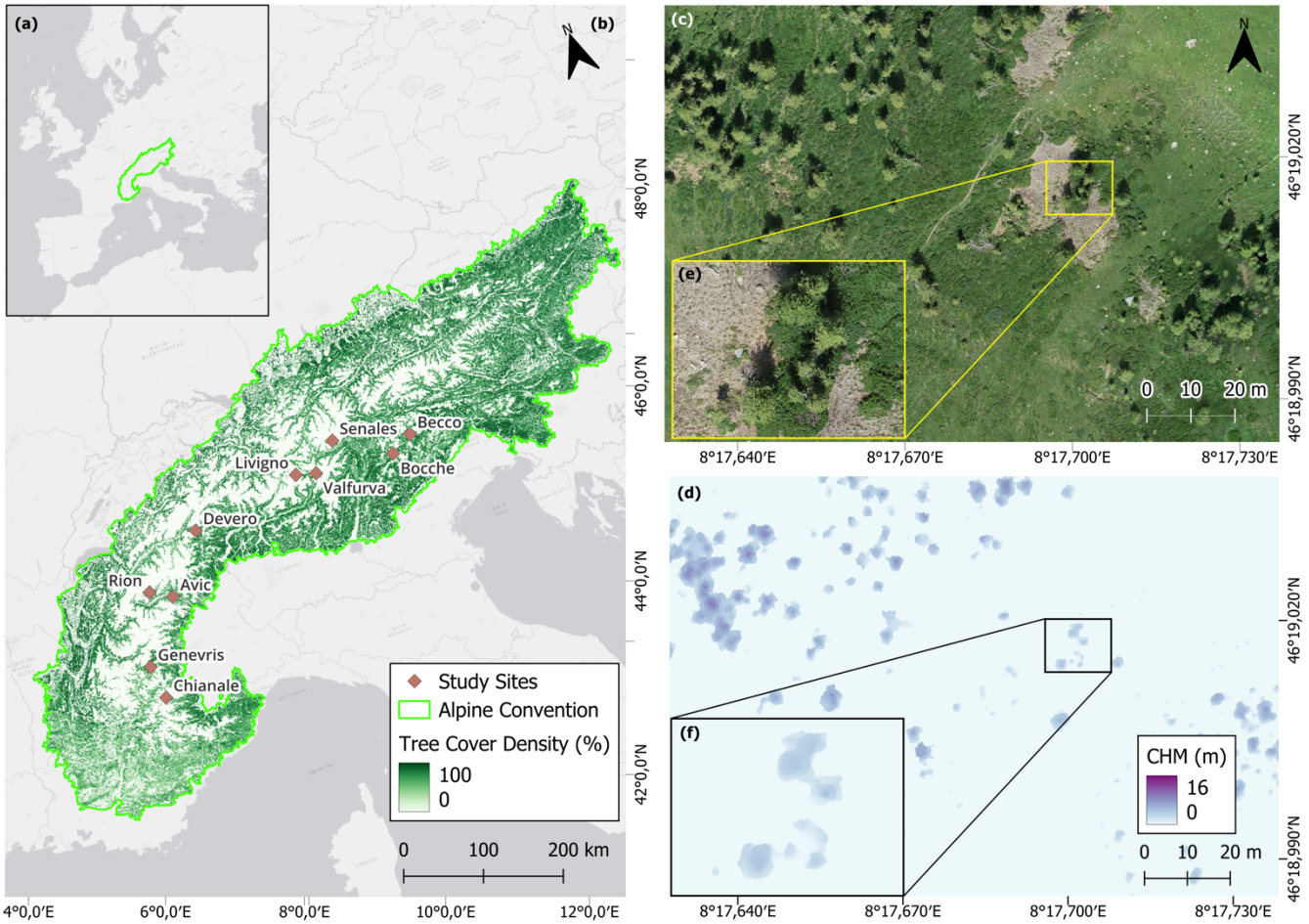

Figure 1. Geographic location of (a) the Alpine Convention Perimeter in Europe and (b) the ten study sites (brown diamonds) along with their names across the Alps. Detail in the UAV-derived orthomosaic of the study site (c) Devero and (d) same site overlayed with the canopy height model (CHM). (e) further details of the study area Devero and (f) its CHM. For further details see Sect. 2.2

Table 1. Details of the study sites including date of the survey, their latitude and longitude (WGS84), average elevation (m a.s.l.), aspect, dominant tree species, mean annual temperature (°C) and total annual precipitation (mm). Climate variables were derived from Chelsa Climate database (Karger et al. 2020), while position, elevation, and species from the field surveys.

Study site	date	Latitude (°)	Longitude (°)	Elevation (m a.s.l.)	Aspect	Species	Mean annual temperature (°C)	Annual precipitation (mm)
Genevris	26/07/2021	45.030	6.897	2,379	W	*L. decidua, P. cembra*	1.4	1263
Chianale	29/06/2021	44.646	6.975	2,283	N	*L. decidua, P. cembra*	1.6	829
Rion	22/09/2021	45.830	7.262	2,290	S-SE	*L. decidua, P. abies*	0.7	1759
Avic	06/10/2021	45.697	7.593	2,184	SE	*L. decidua, P. abies, P. uncinata*	1.9	1115
Devero	14/06/2021	46.316	8.294	2,186	NW	*L. decidua*	1.4	1631
Livigno	22/07/2021	46.516	10.142	2,322	NW	*L. decidua, P. cembra, P. mugo*	0.1	1067
Valfurva	21/07/2021	46.454	10.461	2,371	E	*L. decidua, P. abies, P. cembra*	1.2	894
Senales	07/07/2021	46.727	10.898	2,319	S	*L. decidua, P. cembra, P. abies*	0.2	923
Bocche	06/07/2021	46.338	11.744	2,245	SW	*P. cembra, L. decidua, P. abies*	0.7	1225
Becco	28/09/2021	46.471	12.118	2,190	N-NE	*P. cembra, L. decidua, P. abies*	0.9	1449

2.2 Sampling design and data collection

We selected ten treeline ecotones above 2,000 m a.s.l. along an east-west gradient across the Italian Alps, with a minimum distance of 25 km between sites. Site selection was stratified by administrative region with only fully accessible location included, and edaphic treelines were explicitly avoided. In these ecotones, we placed ten 9-ha square plots (300 m x 300 m) with a side aligned parallel to the steepest slope of the mountainside so that the forestline occurred in the lower third of the plot. We defined forestline as the continuous line separating the closed forest (canopy cover > 10%) from the semi-open and open areas (canopy cover < 10%) (FAO, 1998). The canopy cover was assessed based on the pan-European Tree Cover Density (TCD) layer provided by Copernicus (https://land.copernicus.eu/en).

Data collection included UAV and field surveys in summer 2021. We used a DJI Phantom 4 pro V2 quadcopter equipped with a RGB camera featuring a 1-inch CMOS sensor with 20 MP. Each UAV survey consisted of three flight paths: two of them with the camera in the nadiral position (one aligned along the contour lines and the other perpendicular), and one with an oblique camera perspective of 60° off-nadir, granting a more complete view of trees and terrain features. To mitigate spatial

resolution loss in the lower portion of the plot due to the slope steepness, each set of three flights was repeated from a central position of the plot, at approximately 150 m from the plot side, resulting in a total of six flights per study site. Flight height was fixed at 30 m above the highest point of the 300 × 300 m plot for the first set and above the middle of the study site for the second. All the flights were performed on sunny, windless days to minimise shadowing from clouds and image distortions due to UAV irregular motion. To assess how different phenological stages and light conditions affect canopies detection, we performed UAV flights in Avic and Rion during the late vegetative period and late afternoon, respectively (Table 1). Images were captured with 80% frontal and lateral overlaps to ensure high-quality structure-from-motion outputs. Prior to the UAV flights, 12 ground control points (GCPs) marked with bull's eye targets were placed within the flight area. Their positions were recorded using Trimble R2 and Reach RS2 GNSS (Global Navigation Satellite Systems) antennas, providing both sub-metric horizontal and vertical positioning accuracies with a 10-minute static occupation time. GCP positions were post-processed for a final georeferencing correction. The acquired RGB aerial images were processed using Agisoft Metashape Pro software version 1.5.1. A Structure-from-Motion procedure was employed to generate 3D point clouds, from which we derived digital terrain models (DTMs), digital surface models (DSMs), and orthomosaics with 5-cm spatial resolution. The classification of ground and non-ground points in the point clouds was based on a threshold of 10 cm height: points lower than 10 cm were considered ground and used to produce the DTM. Canopy height models (CHMs) were then produced by subtracting the DTM from the DSM.

In the field, we recorded the position, height, and species of 50 randomly selected individual trees per study site, scattered across the plot. In this study, we defined individual trees as individual tree crowns clearly separable from the other adjacent crowns. Due to its low abundance and specific growth form characteristics (Table 1), dwarf mountain pine was not considered as a tree in our analyses. Tree height was measured using a TruPulse 200b (Crisel srl) or a measuring tape for smaller individuals. Tree positions were recorded using the same GNSS antennas described above, with a 3- to 5-minute occupation time. The final ground-truth dataset included a total of 500 georeferenced trees across the ten sites.

The entire workflow of the study, from data acquisition to final analyses, is reported in Figure 2.

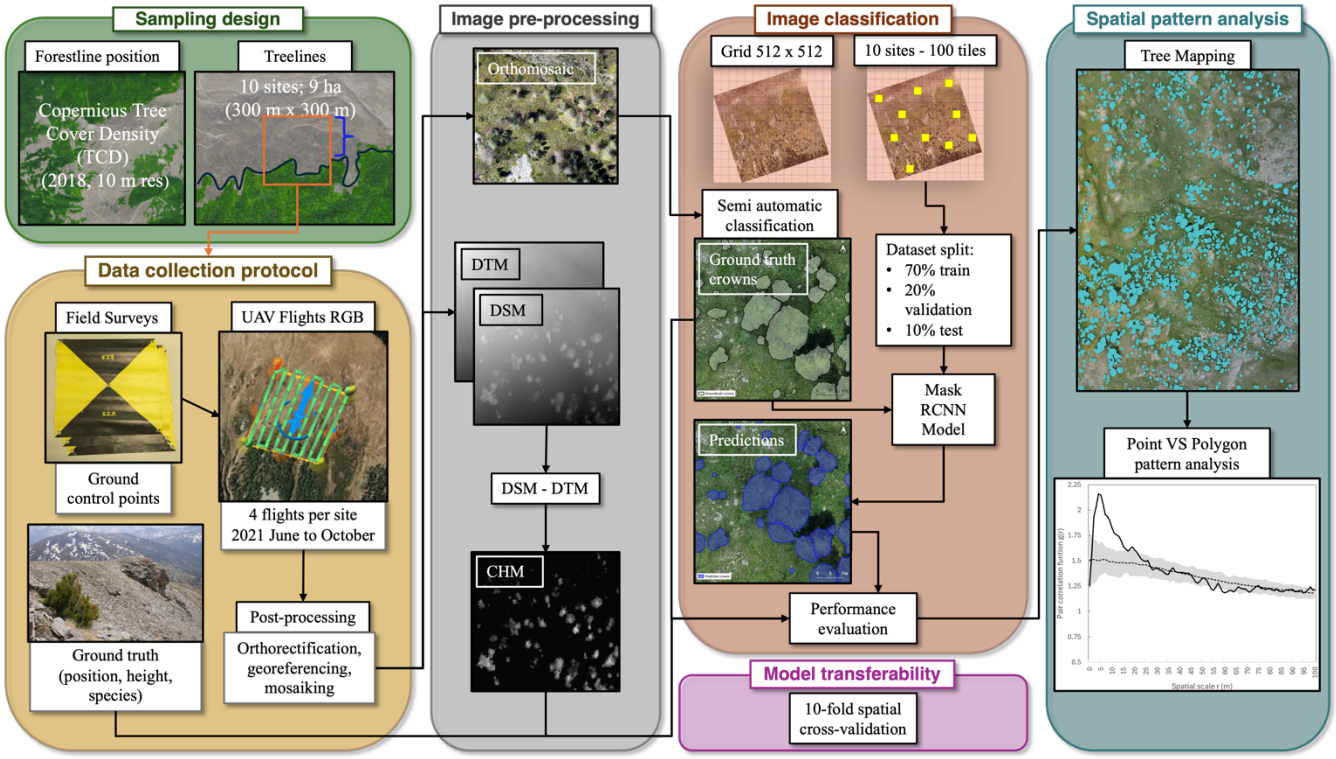

Figure 2. Overview of the workflow adopted to conduct tree-scale analyses at the alpine treeline ecotone. Each box depicts a different methodological step of the study.

2.3 Deep learning modelling

To perform tree detection and segmentation we used a pre-trained deep learning (DL) model based on the Mask R-CNN algorithm implemented in the "Detectron2" library from Meta AI and available at https://github.com/facebookresearch/detectron2. Mask R-CNN is a DL framework which performs instance segmentation by combining semantic segmentation and object detection (Kattenborn et al., 2021). Its framework involves the generation of region of interest proposals by a deep fully convolutional network, and then there is a classification of the object of interest within each generated region proposal. Our methodology consisted of the following steps: i) cropping the RGB orthomosaic of each study site into adjacent tiles of 512 x 512 pixels; ii) systematically selecting 10 tiles per each study site to create the reference dataset; iii) semi-automatic classification of tree crowns; iv) hyperparameter tuning and model calibration using a dataset randomly split into training, validation, and testing subsets; v) performance evaluation; vi) separate validation of model transferability through spatial cross-validation. Each of the steps is furtherly explained in the following chapters. We selected tiles of 512 x 512 pixels (equivalent to 25.6 x 25.6 m at 5 cm spatial resolution) as this size resulted in models with higher detection rates and accuracy across all sites compared to smaller tiles of 128 x 128 and 256 x 256 pixels.

2.3.1 Training, validation, and test data

We here used only 5% of the total amount of tiles for training, with the purpose of testing the limits of using a low number of training images on a pre-trained DL model. To build a strong reference dataset we fine-tuned the model using a Meta AI Segment Anything for the creation of individual ground truth crowns samples (https://github.com/facebookresearch/segment-anything). Annotations were carried out by visual interpretation of RGB images, resulting in non-overlapping binary masks. To minimise operator biases photo interpretation was conducted by a single operator. The semi-automatically delineated ground truth crowns were used to evaluate the model performances in delineating tree crowns (see Section 2.3.3). At the end of the process, we obtained a dataset with a total of 1,016 individual canopies of different coniferous species (larch trees n = 885, pine trees n = 131). All the segmented ground truth crowns were classified and labelled as ”trees" regardless of the species due to the similar spectral information.

To generate the training, validation and test datasets, the reference dataset of 100 tiles (512 x 512) was split into 70 % of images for training, 20 % for validation, and 10 % for testing. The split in the three datasets was performed by systematically sampling the 512-pixel tiles in the reference dataset. The tiles were sampled diagonally in order to cover a larger surface of the study area and to minimise spatial autocorrelation. Finally, we assessed the performance of the model using the test dataset, consisting of tiles with which the model was not familiar. The model trained in this way was used to perform predictions on the rest of the tiles to generate tree maps. However, this type of dataset partitioning does not guarantee model transferability since images from all sites are included in each phase of training, validation, and testing. Hence, we performed a spatial cross validation from start to evaluate model generalizability. A k-fold spatial cross-validation was performed using training and validation datasets partitioned according to their geographic distribution. The dataset was partitioned into ten folds based on study sites. In each iteration, images from nine sites were used for training, while the remaining site's images were reserved exclusively for testing. This procedure was repeated across ten iterations, such that each site served as the test set once, thereby ensuring a leave-one-site-out cross-validation scheme. The outputs of the ten iterations through the entire dataset were finally averaged to achieve a mean F1 score, precision, recall, and average precision (AP) value.

2.3.2 Model development and hyper-parameter configuration

During training we used the Adam optimizer with a learning rate of 0.00025, 128 ROIs per image, 1500 epochs, and a batch size of 30. We used the R101-FPN configuration as it offers a good balance between training speed and segmentation accuracy (https://github.com/facebookresearch/detectron2/blob/main/MODEL_ZOO.md). To prevent overfitting, we monitored the validation loss in the F1-score every 100 iterations and implemented early stopping if the F1-score declined for more than five evaluations. The model was trained with data augmentation consisting in random resizing and rotation of the input images.

We predicted tree crowns contours using the tiling process developed by Ball et al. (2023), which consists of creating a buffer around each tile to avoid splitting crowns located at the edges of the tiles. The overlapping crowns resulting from this operation

were then filtered by removing those with the lowest confidence value assigned during the prediction. Classified maps were then post-processed to reduce noise and correct evident misclassifications. Crowns remaining after this cleaning process were considered valid tree detections. Model evaluation was computed prior to the cleaning process for all the evaluation metrics except detection rate (DET%) and IoU, which were calculated after the post-processing (see Section 2.3.4 for details).

2.3.3 Model performance assessment

To assess the performances of the DL model, we selected four evaluation metrics commonly used in individual tree detection studies (Beloiu et al., 2023; Dersch et al., 2023; Dietenberger et al., 2023; Xie et al., 2024): (i) precision (1), recall (2), F1 score (3), and average precision (4). The F1 score, a measure of test accuracy, is the weighted average of precision and recall; values closer to one indicate higher classification accuracy. The average precision is computed as the area under the precision-recall curve. It evaluates the quality of the classifier in retrieving the relevant instances.

To evaluate model transferability, we corroborated the results with a spatial cross-validation procedure. Metrics (1)-(4) were computed after each cross-validation fold and the results were averaged to achieve a mean estimate.

In addition, tree maps were evaluated in terms of two spatially explicit metrics: detection rate (DET%), and delineation accuracy (IoU). DET% is the ratio between the predicted number of trees and the number of trees measured in the field (5). It is computed to evaluate how many objects were correctly classified out of all the ground truth data. For the evaluation we used only field-sampled trees that did not belong to the training and validation datasets. The IoU is measured as the ratio between the area of overlap and the area of union of the ground truth crown and predicted crown (6), providing an estimate of the segmentation and delineation accuracy. Semi-automatically delineated crowns were used as ground truth for IoU assessment.

$$Precision = \frac{TP}{TP+FP} = \frac{correctly\ predicted\ trees}{all\ trees\ predictions}, \quad (1)$$

$$Recall = \frac{TP}{TP+FN} = \frac{correctly\ predicted\ trees}{all\ ground-truthed\ tree\ predictions}, \quad (2)$$

where TP are the true positives instances; FP are the false positive instances; FN are the false negatives (number of ground truth trees that the model did not detect).

$$F1\ score = \frac{precision * recall}{\frac{precision+recall}{2}}, \quad (3)$$

$$AP = n(R_n - R_{n-1})Pn\ \mathrm{AP}{=}\mathrm{n}{\sum}(\mathrm{Rn}{-}\mathrm{Rn}{-}1){\cdot}\mathrm{Pn}\,, \quad (4)$$

where n is the number of thresholds; Rn is the recall at the n-th threshold; Pn is the precision at the n-th threshold.

$$DET\% = \frac{number\ of\ predicted\ trees}{actual\ number\ of\ trees}, \quad (5)$$

$$IoU = \frac{area\ of\ overlap}{area\ of\ union}, \quad (6)$$

2.3.4 Tree attributes assessment

Tree position estimation accuracy was assessed by comparing the field-collected coordinates of each tree with the centroid coordinates of the corresponding predicted crowns. For height estimation, we compared the value of the CHM at the predicted centroid with the height measured in the field. The evaluation metrics chosen for evaluating the accuracy in tree height and position were root mean square error (RMSE) and mean absolute error (MAE), both calculated in centimetres. RMSE is a standard deviation of prediction errors or residuals (7). The MAE shows how close the ground truth values and predicted values are to each other (8). It is obtained as the average absolute difference between the predicted value and the real value; hence, it gives an overall estimation of the error in terms of standard SI (International System) units. Position accuracy was also evaluated using the Euclidean distance between the centroid of each predicted crown and the corresponding stem position as recorded in the field (9). For tree height estimation accuracy, we also computed the deviation between real and predicted values calculated both in absolute and relative terms. RMSE, MAE, Euclidean distance and tree height accuracy were computed only for correctly predicted trees (n = 343) with the exclusion of the trees that fell within tiles used for training and validation of the neural network (n = 157).

$$RMSE = \sqrt{\frac{\sum_{i=1}^{n}(x_p - x_r)^2}{n}}, \quad (7)$$

$$MAE = \frac{\sum_{i=1}^{n}|x_p - x_r|}{n}, \quad (8)$$

$$Euclidean\ distance = \sqrt{(X_p - X_r)^2 + (Y_p - Y_r)^2}, \quad (9)$$

where *n* is the number of observations; *xp, yp* are the predicted values; *xr, yr* are the actual values.

We tested tree height influence on the results accuracy by grouping trees into three size classes: small (height ≤ 130 cm), medium (130 cm < height ≤ 200 cm), and tall (height > 200 cm). Statistical differences in accuracy among these groups were evaluated using a Wilcoxon test with pairwise comparison. To investigate how the inclusion in the analysis of trees smaller than 50 cm impacted on the position and height estimation accuracies, we conducted a separate analysis excluding individuals shorter than 50 cm (i.e., considering only trees with height > 50 cm).

252 **2.4 Spatial pattern analysis**

253 Tree maps and extracted tree heights were used to investigate tree spatial patterns. We assessed tree distribution patterns by
254 applying a univariate PPA computed through the software Programita (2014) (Wiegand and A. Moloney, 2004). We used a
255 pair-correlation function g(r), a second-order statistic that is non-cumulative and uses only points separated by a distance r,
256 thus allowing the identification of spatial scales where there are significant interactions among points. We analysed patterns
257 across a distance ranging from 0 to 100 m, that is one-third of the width of the study sites (Rosenberg, 2015). The observed
258 univariate patterns were compared with simulation patterns and confidence envelopes generated by a Heterogeneous Poisson
259 (HP) null model. This null model distributes the points (tree centroids from the tree maps) on the study area with a probability
260 proportional to the intensity map but relaxes the assumption of complete spatial randomness and allows the intensity of the
261 point pattern to vary across the study area. For the generation of the intensity function to be employed in the HP null model
262 we employed an Epanecnikov kernel with enabled edge correction and we set the ring width of the moving window to 5, and
263 allowed only one point per cell.
264 To test significant departure from the null model, for each analysis we performed 99 Monte Carlo simulations which generated
265 99% confidence limits (Carrer et al., 2018; Getzin et al., 2006; Petritan et al., 2015). The spatial pattern was defined as
266 randomised, clustered or regular if the g(r) values were respectively equal, greater or lower than the confidence envelopes
267 calculated using Monte Carlo simulations at specific spatial scales. To verify the robustness and significance of the departure,
268 and to avoid incurring in Type I error (if the value of g(r) is close to a simulation envelope the null model may be rejected even
269 if it is true) we used the Goodness-of-Fit (GoF) over the given distance interval (Loosmore and Ford, 2006).
270 Additional univariate PPAs were also performed for each tree size category in order to gain insights on tree spatial distribution
271 within each dimension class.
272 To assess the relationship existing between tall and small trees we applied a bivariate point pattern analysis (Wiegand e A.
273 Moloney 2004). We extended the pair-correlation function used before for a bivariate analysis (*g12(r)*), thus allowing us to
274 detect the interactions between the two different classes of trees. The interaction was defined as independent, attraction or
275 repulsion if the *g12(r)* values were respectively equal, greater or lower than the confidence envelopes at specific spatial scales.
276 For the bivariate analysis we used the antecedent condition null model, with points of pattern 1 (tall trees) fixed, and points of
277 pattern 2 (small trees) distributed in accordance with a HP null model, where small trees are randomly distributed in the
278 neighbourhood of the tall trees.
279 To investigate potential dynamics of attraction/repulsion among individuals of different sizes we performed the analysis by
280 using the same classes (tall, medium and small trees) previously created. The middle class was used as a dividing element
281 between tall and low trees in order to avoid overlapping groups, and was hence not used in the analysis.
282 One of the assumptions of the PPA is that objects (trees) are considered as points. However, we decided to test whether the
283 point approximation (canopies centroids) was somehow hindering the spatial relationships between trees. To investigate this

aspect all the above mentioned analyses were performed again using as input data the crowns' shapes taken from the generated tree maps, hence using the setting for objects of finite size and real shape (Wiegand et al., 2006). Univariate and bivariate analyses on points approximation and on objects of finite size and real shape were performed for each site using the same settings and were ultimately combined with the "combine replicates" protocol.

3 Results

3.1 Tree detection rate, delineation performances and transferability of the protocol

Throughout the evaluation process, the DL model achieved an F1 score of 0.76, precision of 0.92, recall of 0.79, and AP of 0.68. Spatial cross-validation confirmed the DL model generalizability to yet-unseen data, yielding an F1 score 0.68, precision of 0.90,recall of 0.56, and AP of 0.36 (appendix B).

According to DET% results, the DL model detected 67% of all the trees sampled in the field not included in the training and validation datasets (Table 2). Detection performance was lower for small trees, with a mean detection rate of 52%. As expected, limiting the analysis to trees taller than 50 cm (DET% ab50) led to higher detection rates, resulting in a DET% = 70, thus confirming that smaller trees have a strong negative effect on the detection rate. When considering only tall trees (>200 cm) we reached a mean detection rate of 86%, furtherly supporting the effect of size on detection rates. Among the study sites, Genevris was the site in which the best detection rates were registered (93% for trees taller than 50 cm), followed by Valfurva, Devero, Bocche and Livigno, where the model correctly detected more than 78% of all the trees. IoU results also showed a similar pattern, with tall trees achieving the best performances (IoU = 0.85). Medium and small trees achieved a mean IoU value of 0.73 and 0.69, respectively. The difference between tall trees' IoU and the other two classes' one was significantly different, as confirmed by a Wilcoxon test (Fig. 4a).

Table 2. Single site detection rates and number of total predicted trees (n. pred trees) out of the totality of trees sampled in the field (n. test trees). DET% all = detection rate on the totality of individuals; DET% small = detection rate on small trees; DET% medium = detection rate on medium trees; DET% tall= detection rate on tall trees; DET% ab50 = detection rate on individuals taller than 50 cm.

site	n. test trees	n. pred trees	DET%				
			all	small	medium	tall	ab50
Avic	42	14	33	12	56	75	37
Becco	45	31	69	58	69	85	71
Bocche	50	35	70	48	85	93	79
Chianale	51	32	63	43	73	68	63
Devero	40	33	83	71	86	94	83
Genevris	40	37	93	86	1.00	92	93
Livigno	50	39	78	85	63	89	78
Rion	45	24	53	18	78	93	57
Senales	47	24	51	16	40	83	58
Valfurva	49	40	82	84	76	86	82
Mean	/	/	**67**	**52**	**73**	**86**	**70**

3.2 Tree attributes estimation

The proposed method demonstrated that it was possible to accurately estimate tree positions and height. Trees' predicted position achieved a RMSE of 0.59 m and a MAE of 0.49 m. For most of the predictions, the Euclidean distance between predicted and reference points was less than one metre, with the majority of values around 30 cm (Fig. 3b). Interestingly, position accuracy increased with reducing tree height, resulting in lower deviation values for the two smaller classes (medium and small trees) (mean Euclidean distance value of 0.40 and 0.44 m, respectively; Fig. 4b). The Wilcoxon test highlighted a significant difference between the two smaller classes' results and the one obtained for tall trees, for which the mean Euclidean distance value was 0.61 m.

In regard to height estimations, despite some outliers, we observed a strong ($R^2 = 0.87$) linear relationship between predictions and ground-truths (Fig. 3c). The coefficient of determination, the RMSE of 91.6 cm, and the MAE of 71.8 cm confirm that the SfM-derived point cloud can be used to accurately estimate tree heights. Nearly all height predictions deviated by less than

one metre from ground truth values, with the most frequent relative deviation around 20 cm (Fig. 3d). Prediction accuracy increased with tree height: tall trees had the lowest mean deviation (0.23 m), followed by medium (0.47 m) and small trees (0.62 m) (Fig. 4c).

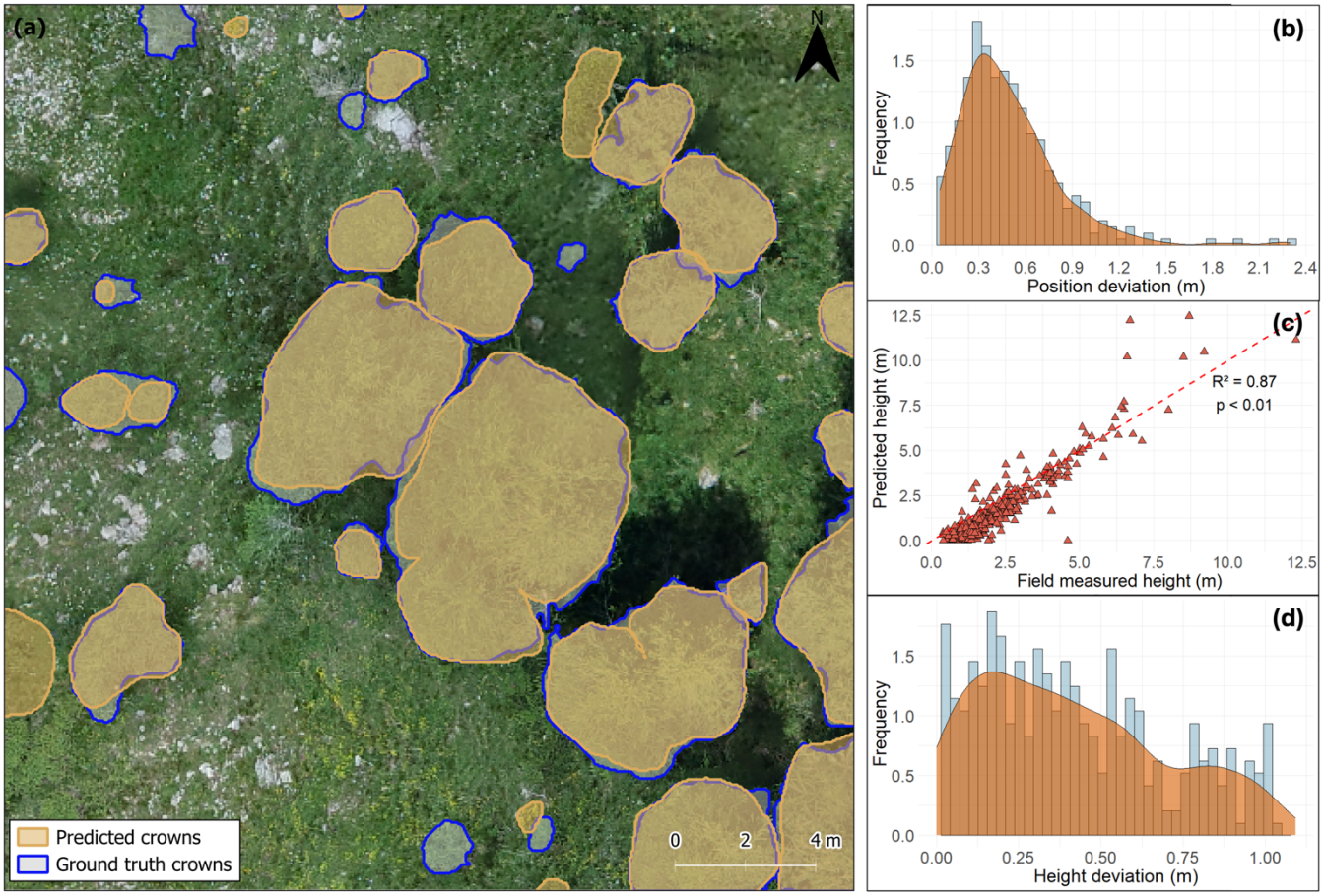

Figure 3. (a) Instance segmentation output with a comparison of crowns predicted by the model (shaded with orange outline) and manually delineated ground truth crowns (shaded with blue outline) in Genevris study site. The image illustrates how smaller trees were harder to detect by the model, with some missing segmentations. Kernel density distribution of (b) relative deviation for position estimation and (d) deviation for height estimations with the smoothed, continuous approximation of the kernel-density estimate in orange. (c) Linear regression model between the field-measured crown heights and estimated heights in metres. The red dashed line represents the 1:1 line.

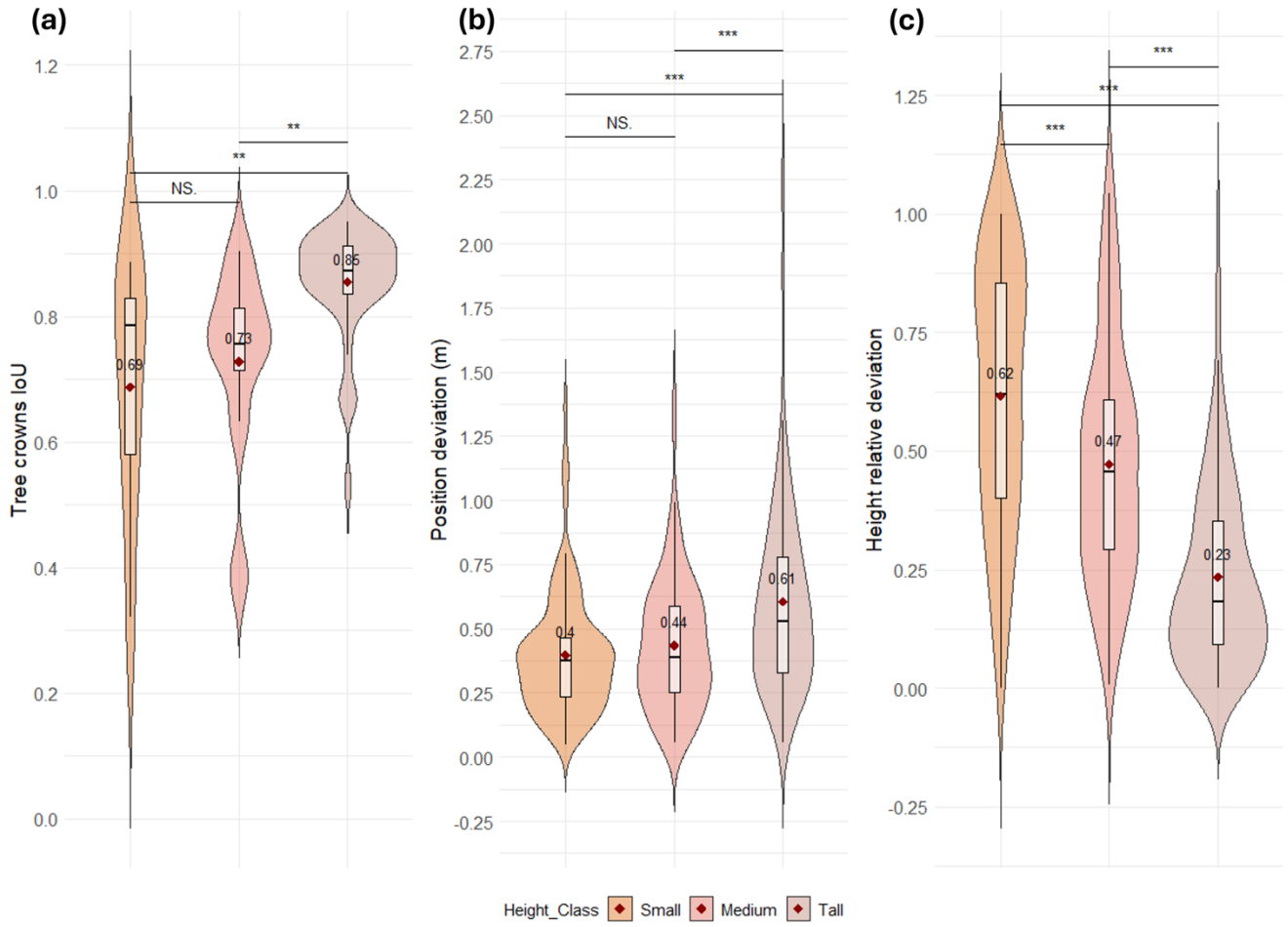

Figure 4. Comparison of model performance for three tree-height classes (Small: ≤ 130 cm; Medium: >130 cm and <=200 cm; Tall: > 200 cm) in predicting trees (a) canopy surface and shape, measured as Intersection-over-Union (IoU) between predicted and reference crown polygons, (b) position deviation, measured as Euclidean distance (m) between predicted and reference tree centroids and, (c) height relative deviation, measured as absolute difference between predicted and reference height divided by the reference height. Violin plots width at a given value shows the kernel-density estimate of the distribution; the overlaid boxplot displays the interquartile range with the median (black line) and mean (dark-red diamonds). Statistical significance (pairwise Wilcoxon tests) is indicated as: NS = not significant; * $p < 0.05$; ** $p < 0.01$; *** $p < 0.001$.

3.3 Treeline spatial patterns and tree-tree interactions

The univariate analysis resulting from the "combine replicates" protocol using tree crown centroids revealed a strong aggregation across all study sites (Fig. 5a). At spatial scales < 20 m, there was a marked positive departure from the pair-correlation function indicating clustering, which turned into a random pattern at 21 m under the HP null model (GoF: $p < 0.05$

in all sites). For spatial scales > 35 m, a slight negative departure from the null model suggested a tendency toward regular distribution. When considered separately, all the ten sites showed similar patterns consistent with the combined result (see details in appendix C). The univariate analysis conducted on tree crown polygons showed slightly different results (Fig. 5b). Despite the overall results indicated a clumped pattern throughout the entirety of the sites, it appears that the clustering occurred for all spatial scales from 0 to 100 m. To understand whether clustering occurred also within size classes, we performed univariate PPAs for all the tree size classes (i.e., small, medium, and tall) separately. The results highlighted a clear trend in forming groups at small spatial scales, among trees of the same size classes (Appendix E).

The 'combine replicates' protocol applied to the bivariate analyses of tree crown centroids revealed a strong spatial repulsion of small trees relative to tall trees across all examined spatial scales (Fig. 5c). Again, by analysing each site separately, they all showed similarities among each other and with the combined replicate result (see details in Appendix D). The bivariate analysis conducted on objects of finite size and real shape (tree crown polygons) led to similar results (Fig. 5d), suggesting the existence of a strong repulsion between small and tall trees.

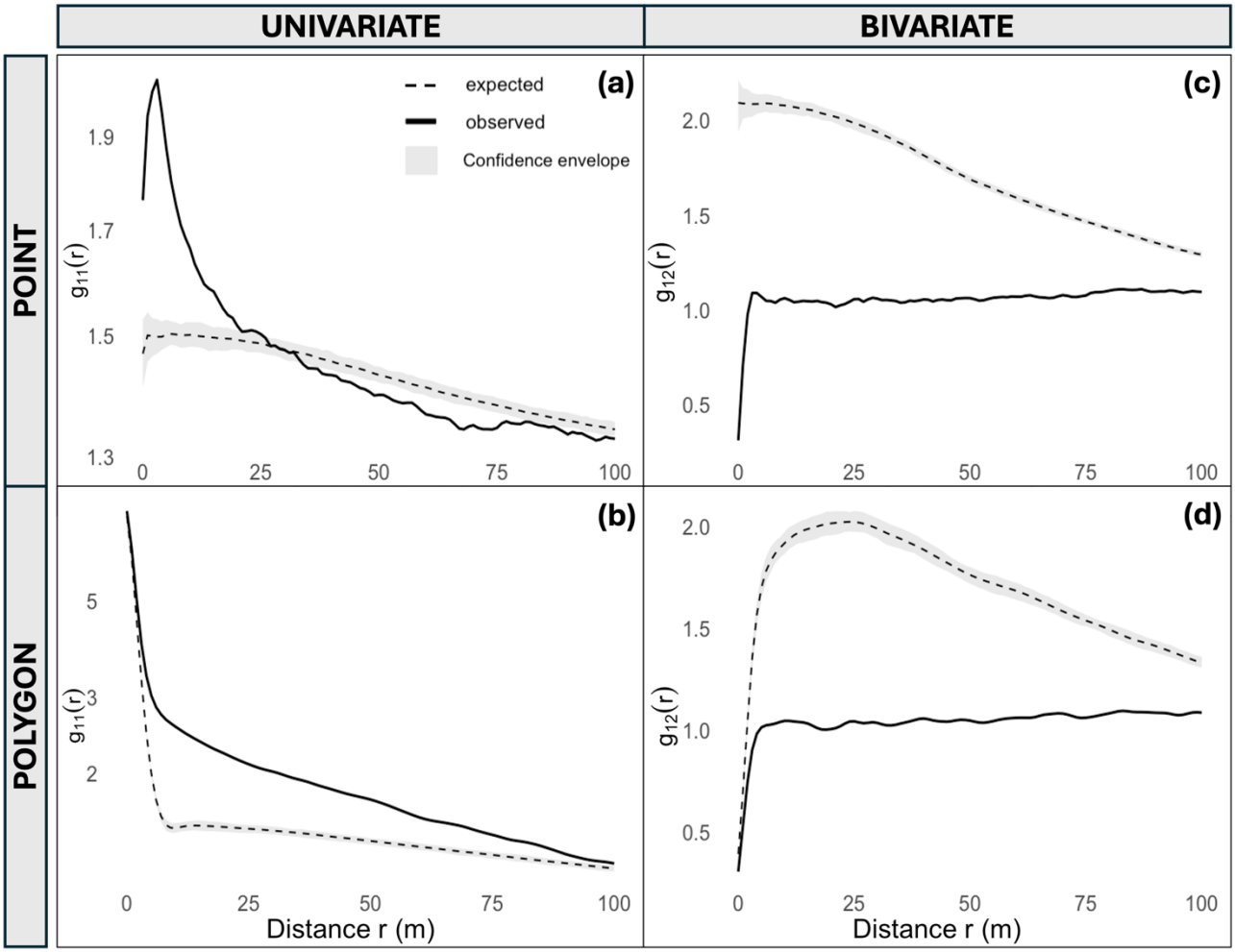

Figure 5. Univariate pair-correlation function g11(r) for (a) centroids and (b) crown polygons. The analysis allows for the definition of a spatial pattern as clumped, random or regular (hyperdispersed) if the summary statistics (black continue line) value is greater than, within, or lower than the confidence envelope (light grey area). The confidence envelope lines represent the upper and lower 95% simulation envelopes. Black dashed lines indicate the expected pattern if the points showed a random spatial distribution. Correlation analysis of tall trees and small trees for (c) centroids and (d) crown polygons. Values of the g12(r) function that significantly deviates from the null model indicate a significant attraction (if positive) or repulsion (if negative) between the two patterns.

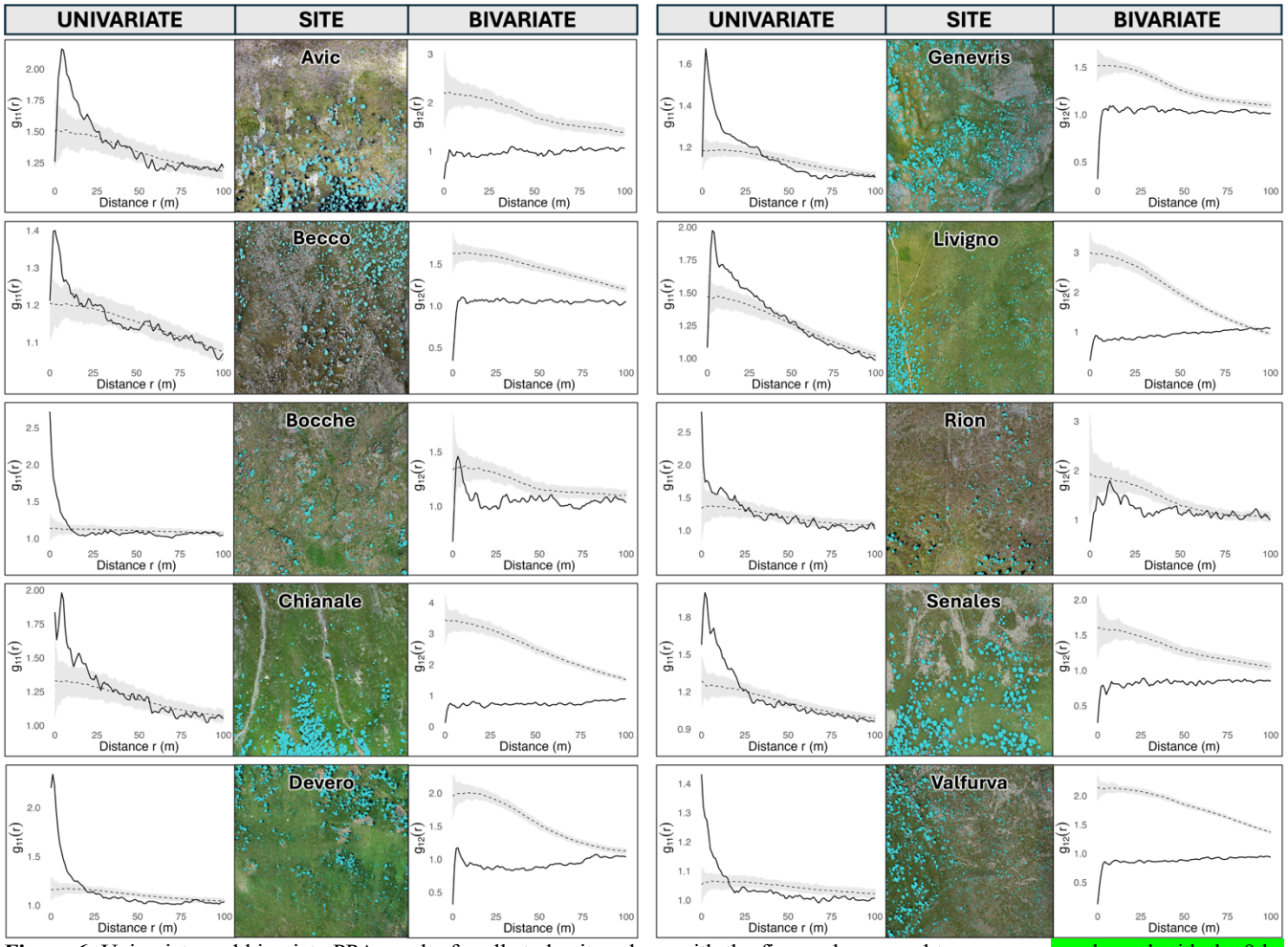

Figure 6. Univariate and bivariate PPA results for all study sites along with the fine-scale mapped tree crowns overlapped with the 9 ha orthophoto as a background image.

4 Discussion

4.1 Detection performances

We demonstrated that RGB imagery from low-cost UAVs can be effectively used for accurate tree detection across large, heterogeneous areas at elevational treelines. Previous studies have conducted similar analyses employing different segmentation strategies in various forest types. Our model achieved precision and recall values that surpass those reported in other studies (Beloiu et al., 2023; Dietenberger et al., 2023). The average IoU across different tree size classes was 0.76, lower than results from plantation-based studies (Hao et al., 2021), but superior to those from mixed temperate forests (Dietenberger

et al., 2023). Regarding detection rates and F1 scores, our results fell within the typical range reported in comparable research (Table 3).

However, direct comparisons with other studies are challenging due to substantial differences in forest types, UAV data acquisition protocols, flight parameters, and the image classification algorithms employed. While our analysis outperformed others on certain metrics, it is important to note that our study was conducted in an environment where individual tree detection is facilitated by the reduced presence of intertwined canopies, unlike in tropical or temperate forests. Conversely, this advantage was offset by the inclusion of small trees in our analysis, a factor that negatively impacted the results and is often excluded in similar studies.

Table 3. Performances of recent studies focused on tree detection and crown delineation in forest ecosystems using UAV-derived data. DET% = detection rate on the totality of individuals; IoU = Intersection over Union; AP = Average Precision.

reference	Forest type	sensor	crown detection algorithm	DET%	precision	recall	F1-score	IoU	AP
Present Work	mixed open woodland	RGB	Faster R-CNN	70	0.92	0.79	0.76	0.76	0.68
Beloiu et al. (2023)	mixed temperate forest	RGB	Faster R-CNN	-	0.75	0.78	0.76	-	-
Dietenberger et al. (2023	mixed temperate forest	RGB	Region growing	-	0.68	0.61	0.64	0.44	-
Weinstein et al. (2019)	mixed open woodland	RGB, LiDAR	RetinaNet	82	-	-	-	-	-
Xiang et al. (2024)	several forest types	LiDAR	3D CNN	-	-	-	0.85	-	-
Dersch et al. (2023	coniferous, deciduous, mixed stands	LiDAR	Mask R-CNN	-	-	-	0.86	-	-
Jing et al. (2012)	mixed forests	LiDAR	Multi-scale analysis , Marker-controlled watershed segmentation	69	-	-	-	-	-
Ball et al. (2023)	tropical forests	LiDAR	Mask R-CNN	-	-	-	0.64-0.74	-	-
Xie et al. (2024)	Chinese fir plantation	RGB	Mask R-CNN	-	-	-	-	-	0.55
Hao et al. (2021)	Chinese fir plantation	RGB	mask R-CNN	-	-	-	0.85	0.91	-

We hypothesized that tree height would significantly influence model performance. By categorising trees in different size classes, we were able to track detection performance, confirming that accuracy improves with tree size across all study sites. In all the study sites, detection was high for taller trees (86%) but dropped for smaller ones (52%), confirming our hypothesis. In addition to being inherently more challenging to detect in the imagery due to their diminished size, smaller trees often present altered lighting conditions due to being partially obscured or completely concealed by taller ones (Beloiu et al., 2023; Dietenberger et al., 2023; Hamraz et al., 2017), leading to missed detections (i.e., false negatives). This problem is exacerbated

in dense clusters (Vauhkonen et al., 2012), common in most of our study sites. Another critical challenge in tree detection is the blending of canopies colours with the background, a factor that largely depends on the tree, shrub, and herbaceous species on the site (Diez et al., 2021; Weinstein et al., 2019). Here, although the problem also affects tall trees, it was markedly more problematic for smaller ones.

Despite recent advancements in AI tools for object detection and segmentation, accurately identifying small trees in RGB images over large and complex areas is still in its infancy. Moreover, such improvement would remain unfeasible without significantly lowering flight height, which results in increasing extended survey times in mountainous terrain (Fromm et al., 2019). Nevertheless, due to the harsh environmental conditions at the treeline ecotone, long-term survival of small trees is jeopardised by factors such as unsuitable sites for survival (Davis and Gedalof, 2018; Marquis et al., 2021), failure to grow in harsh conditions (Crofts and Brown, 2020; Frei et al., 2018; Müller et al., 2016) and predation (Brown and Vellend, 2014; Cairns et al., 2007). Thus, while the precise mapping of small trees may be of secondary importance compared to taller, potentially permanent trees when evaluating survival rates and seed distribution, small trees are crucial when investigating the encroachment process.

With the present work, we investigated how unique treeline characteristics influenced model performance. At the Mont Avic treeline, where European larch is the dominant species, we tested the leaf-off effect on detection rate. Scarcity of green needles on the canopies resulted in lower performances (Table 2). This finding is consistent with previous studies underscoring how leaf-off season surveys are often correlated with lower detection accuracies (Imangholiloo et al., 2019).

The poor cross validation results from the Rion site highlight the substantial influence of illumination conditions on detection performances. As noted by Diez et al. (2021), low sun angles lead to variations in canopy color and the formation of long, distorted shadows, which can significantly impair detection accuracy.

These results reveal some of the main limitations of RGB-based approaches, underscoring the need of applying a standardised sampling protocol throughout all the study sites to augment results reliability or provide more input data to increase variability in the training dataset.

With the exception of Rion and Avic, a clear waning trend in tree detection related to a specific terrain feature of the site - presence of rocks (Becco), herbaceous species (Chianale) or others - was not found. These findings suggest that terrain characteristics had a negligible effect on detection rates, supporting the generalizability and transferability of the approach to treeline environments with differing features.

4.2 Tree attributes estimation and transferability of the protocol

The proposed approach has demonstrated the ability to accurately georeference individual trees (RMSE = 0.59m; MAE= 0.49m) and estimate their height (RMSE = 91.6 cm; MAE = 71.8 cm); some of the observed deviations may in fact be attributable to inaccuracies in the ground control data rather than the UAV images. Despite the high precision of the GNSS antenna employed, some small georeferencing errors are inevitable (e.g. due to limited sky view, positional accuracy can be

limited). Additionally, during field surveys, GNSS points coordinates of tree locations are recorded near the base of the tree rather than directly below the real treetop, introducing further spatial errors (Shimizu et al., 2022; Vauhkonen et al., 2012). Nevertheless, our tree position estimations were highly satisfying and comparable with results obtained in other recent studies employing similar or more sophisticated gears in environments with analogous open stands. For instance, Castilla et al. (2020) georeferenced coniferous species in a boreal forest using SfM point clouds achieving an RMSE of 20 cm, while Fernández-Guisuraga et al. (2018) extracted tree position of coniferous species in a post-fire environment attaining a RMSE < 30 cm.

Tree height estimations presented a trend skewed towards underestimation (Fig. 3c), an issue attributable to the low sharpness of the DSM generated through SfM, as also evidenced by Panagiotidis et al. (2017) and Wallace et al. (2016). Airborne laser scanning is the most well-known tool for DTM modelling due to its better capability in penetrating tree crowns, which often result in highly accurate estimation of tree features. However, in the present study we provide evidence that by means of photogrammetric point clouds it is possible to extract tree height with an accuracy comparable to that achieved using LiDAR sensors, which are still moderately expensive, thus limiting the feasibility of repeated surveys in many cases. Coops et al. (2013) assessed tree height over a Swiss treeline ecotone by employing LiDAR sensors with an RMSE of 0.70 m. Studies employing LiDAR technologies in boreal treelines documented a standard deviation of 0.11–0.73 m (Næsset and Nelson, 2007) and of 0.16–0.57 m (Næsset, 2009). Using LiDAR, Wallace (2012) reported a mean height standard deviation of 0.24 m in a stand with sparse trees—a level of precision that clearly surpasses our results. However, when compared to studies using SfM point clouds for tree height estimation, our results demonstrate higher accuracy. For instance, Wallace et al. (2016) compared LiDAR and SfM-derived point clouds in a stand with spatially variable canopy cover, finding RMSE values of 0.92 m and 1.30 m, respectively—the latter being higher than ours. Similarly, Brieger et al. (2019) estimated tree heights in an open larch forest and reported a mean RMSE of 1.42 m, further supporting the comparatively greater accuracy of our photogrammetric approach for tree height estimation in open stands.

4.3 Spatial patterns and tree interactions in the Italian alpine treeline ecotone

Several recent studies have highlighted how tree spatial patterns vary along an elevational gradient within the treeline ecotone (Garbarino et al., 2020; Jia et al., 2022; Wang et al., 2021). Other works have investigated tree recruitment at different sites at broad spatial scales (Nicoud et al., 2025), and others investigated spatial patterns on multiple sites in the Pyrenees (Birre et al., 2023). However, to the best of our knowledge, there are no previous studies that have simultaneously investigated the patterns of multiple treelines at the same level of spatial extent (90 ha) and resolution (5cm) as presented in this work.

We found a discrepancy between the univariate analysis performed on centroids (point approximation) and tree crowns (polygons). The dissimilarities are potentially due to a systematic effect in the size of the objects (Wiegand personal communication). First of all, the polygon pattern analysis uses more data points (each cell belonging to an object is counted as a point), and therefore it is possible that the range of significant effects is larger. Furthermore, it is possible that having larger

447 objects in a region of the observation window, as it is common in our study areas, may result in a greater clumping across the
448 analysed spatial scale. Such differences in polygon and point summary functions have already been found in previous studies
449 and are believed to be due to ecological processes (i.e. competition) instead of methodological bias (Vacchiano et al., 2011).
450 Whether the cause is one or another has to be further investigated.
451 Despite the discrepancy on the spatial scale, univariate PPA results revealed a tendency towards a clustered horizontal structure
452 among all trees within our study areas. This is the typical behaviour within the sub-alpine altitudinal belt, as also consistently
453 found in other studies conducted on elevational treelines in Europe (Beloiu and Beierkuhnlein, 2019), USA (Garbarino et al.,
454 2020) and China (Jia et al., 2022). Human impact has been the major driving force in shaping the investigated treelines,
455 affecting patterns and reciprocal patterns of mature and young individuals. However, over the last few decades, the
456 abandonment of remote areas has led to a decrease in human activities such as grazing and silviculture (Anselmetto et al.,
457 2024). As a consequence, recolonization processes driven by natural dynamics have become more important.
458 Various researchers emphasise how terrain features such as microtopography and soil spatial patterns can significantly
459 influence tree distribution at the treeline (Feuillet et al., 2020; Marquis et al., 2021; Müller et al., 2016). The great heterogeneity
460 of terrain inherent to alpine treelines generates a great diversity of microsites, resulting in a mosaic of favourable and
461 unfavourable microsites (Davis and Gedalof, 2018; Marquis et al., 2021). Owing to this, trees can be rather diffuse on a
462 favourable area but also clustered in small groups where better chances of survival are found. In addition to topography,
463 competition and facilitation dynamics between tree species may exert an important role on the evolution of the treeline ecotone.
464 The results of our bivariate tree-tree interaction analysis showed a repulsion between small – potentially younger – and tall -
465 potentially older - trees at all the analysed spatial scales.
466 The abrupt spatial segregation between tall and small trees suggests that tree establishment dynamics within the studied areas
467 are potentially driven by inter-size class competition, and intra-size class facilitation, with small trees favouring sites far from
468 existing clusters of tall trees. Furtherly underpinning this hypothesis is the results of the univariate PPA for the separated size
469 classes, which show how trees belonging to the same size class are organised in clusters in the landscape. How biotic
470 interactions may play a dominant role in driving treeline encroachment dynamics has been discussed in previous studies
471 (Callaway, 2002; Frei et al., 2018; Neuschulz et al., 2018). It is broadly known that in temperature limited environments tree
472 patches can improve microsite conditions, by influencing snow thickness, soil properties, microclimate and offering physical
473 support and protection from herbivores (D'Odorico et al., 2013; Germino et al., 2002). These positive effects, however, can
474 be offset by competition for vital resources such as light, soil moisture and nutrients (Frei et al., 2018; Moir et al., 1999), which
475 ultimately hinders seedling growth and survival. Although our bivariate analysis result suggests the presence of inter-class

competition in high-elevation environments in the Alps, and is in line with previous studies findings (Carrer et al., 2013), further analyses are needed to advance our understanding of the effects of biotic interactions on tree spatial pattern at the treeline.

4.4 Limits and perspectives

Our results demonstrate that combining low-cost UAV and sensors with open-source AI libraries enables accurate fine-scale mapping and extraction of individual attributes. Our detection rates were comparable or superior to many other DL-based classification studies in natural forests. However, recognising small individuals with high accuracy in RGB images remains a challenge. As highlighted in recent scientific literature, LiDAR-informed segmentation approaches could provide a valuable alternative for comprehensive mapping of individual trees, filling the gap left by our methodology. Another crucial feature of great importance for many ecological analyses is the species composition of the community. The use of multi or hyperspectral sensors would solve this issue by enabling the classification of tree species and thus the analysis of species composition, interactions among individuals, and spatial patterns of individual and interacting species. Alternatively, species-level analyses are also possible with very-high-resolution RGB images acquired through low-elevation UAV flights achieving a very fine ground sampling density (~ 1.6 cm/px (Egli and Höpke, 2020)), as they can reveal species-specific crown architecture and morphology.

Due to their dynamic nature, it is of great importance to study treeline ecotones in long-term monitoring research. For this task, we envision future research activities to apply the presented approach to simultaneously map and detect tree species at the treeline. The final goal is creating a global network of accurately mapped treeline datasets to monitor the effects of global change on treeline dynamics and explain the position and pattern of the treeline at different scales.

5 Conclusions

We tested the performance of a Mask R-CNN deep learning model in capturing single-tree attributes across sprawling, remote, and heterogeneous treeline ecotones, using UAV-derived structure-from-motion point clouds. UAV employment allowed us to conduct surveys in a more labour and time efficient manner compared to traditional ground-based methods while also increasing the spatial extent of the study area. This enhanced the reliability of ecological inference on treeline processes. Our results showed that the proposed approach can effectively produce fine-scale tree maps over 90 ha of treeline ecotones. The model successfully identified 70% of trees taller than 50 cm and 86% of trees taller than 2 m across the ten study sites in the Italian Alps. Beyond its success in detecting tree crowns, the approach also performed well in delineation tasks. We

demonstrated the potential of applying the resulting dataset in treeline ecology by analysing spatial patterns and interactions among trees of different size classes.

The present work underpins the possibility of using UAVs to advance treeline research, bridging the gap left by limited-in-scale and labor-intensive field surveys and less accurate satellite imagery. The ability to achieve such results with the low-cost equipment used in this study, combined with the flexibility of the protocol to site-specific conditions with minimal data preparation requirements, makes this approach both accessible to a wide range of scientists and forest managers and reliable. These features showcase the methodology as a valuable tool for several applications in forest assessment, ecological restoration, and conservation planning.

Appendix A:

Figure A1. Detail in the UAV-derived orthomosaic of (a) Avic, (b) Becco, (c) Bocche, (d) Chianale, (e) Devero, (f) Genevris, (g) Livigno, (h) Rion, (i) Senales and (j) Valfurva.

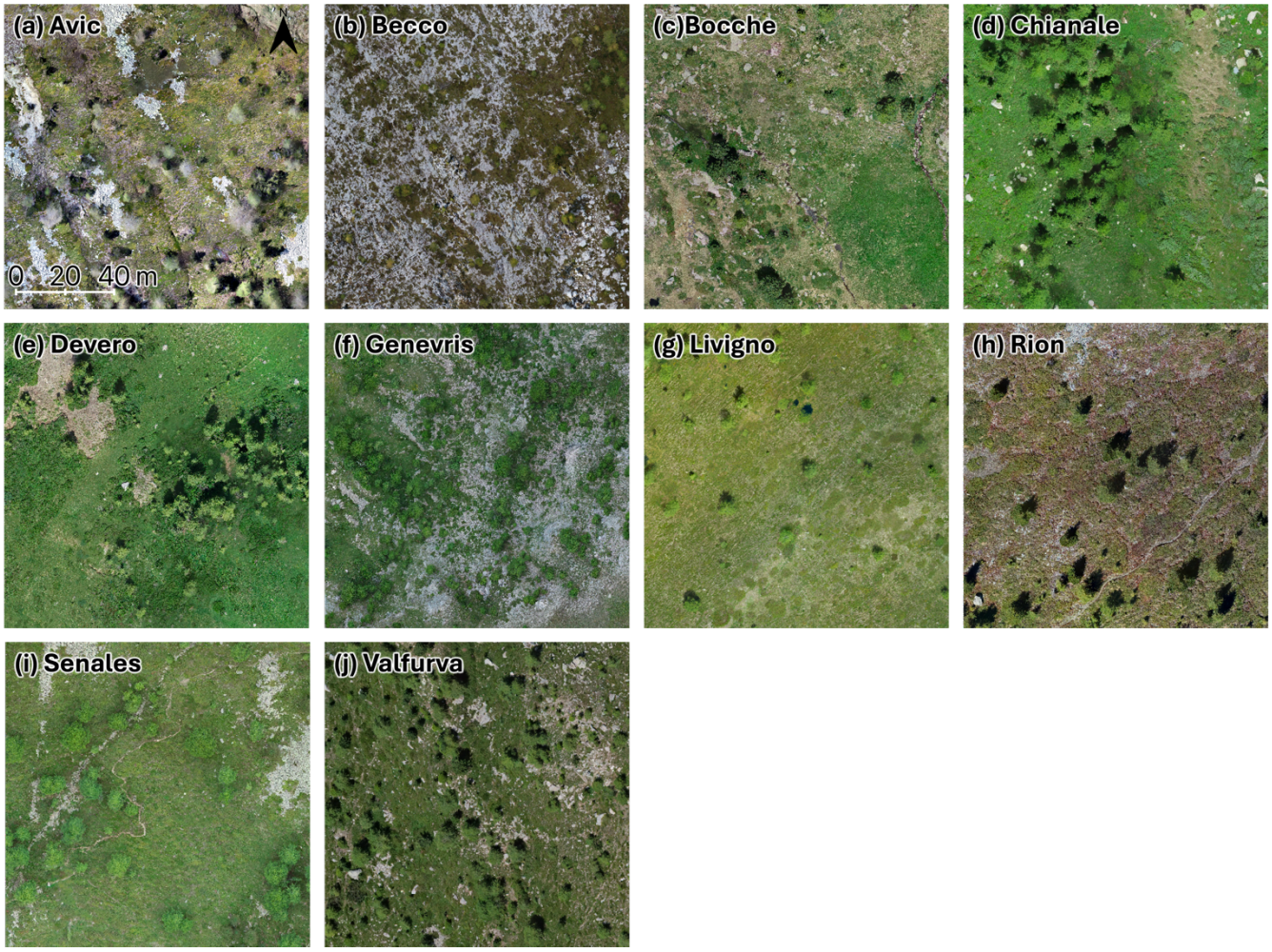

Appendix B:

Table B1. Results of spatial cross-validation analysis.

site	***F1-score***	***precision***	***recall***	***AP***
Avic	0.60	0.83	0.48	0.14
Becco	0.81	0.80	0.87	0.45
Bocche	0.48	1.00	0.35	0.34
Chianale	0.73	0.85	0.40	0.36
Devero	0.63	0.93	0.54	0.27
Genevris	0.76	0.97	0.66	0.45
Livigno	0.78	0.94	0.50	0.58
Rion	0.62	1.00	0.50	0.34
Senales	0.60	0.88	0.49	0.41
Valfurva	0.78	0.76	0.84	0.32
Mean	**0.68**	**0.90**	**0.56**	**0.37**

Appendix C:

Figure C1. single sites' results of the univariate pair-correlation function g11(r) in (a) Avic, (b) Becco, (c) Bocche, (d) Chianale, (e) Devero, (f) Genevris, (g) Livigno, (h) Rion, (i) Senales and (j) Valfurva using point approximation. The confidence envelope (light grey area) represents the upper and lower 95% simulation envelopes. The found spatial pattern is considered clumped, random or regular (hyperdispersed) if the summary statistics (black continue line) value is greater than, within, or lower than the confidence envelope.

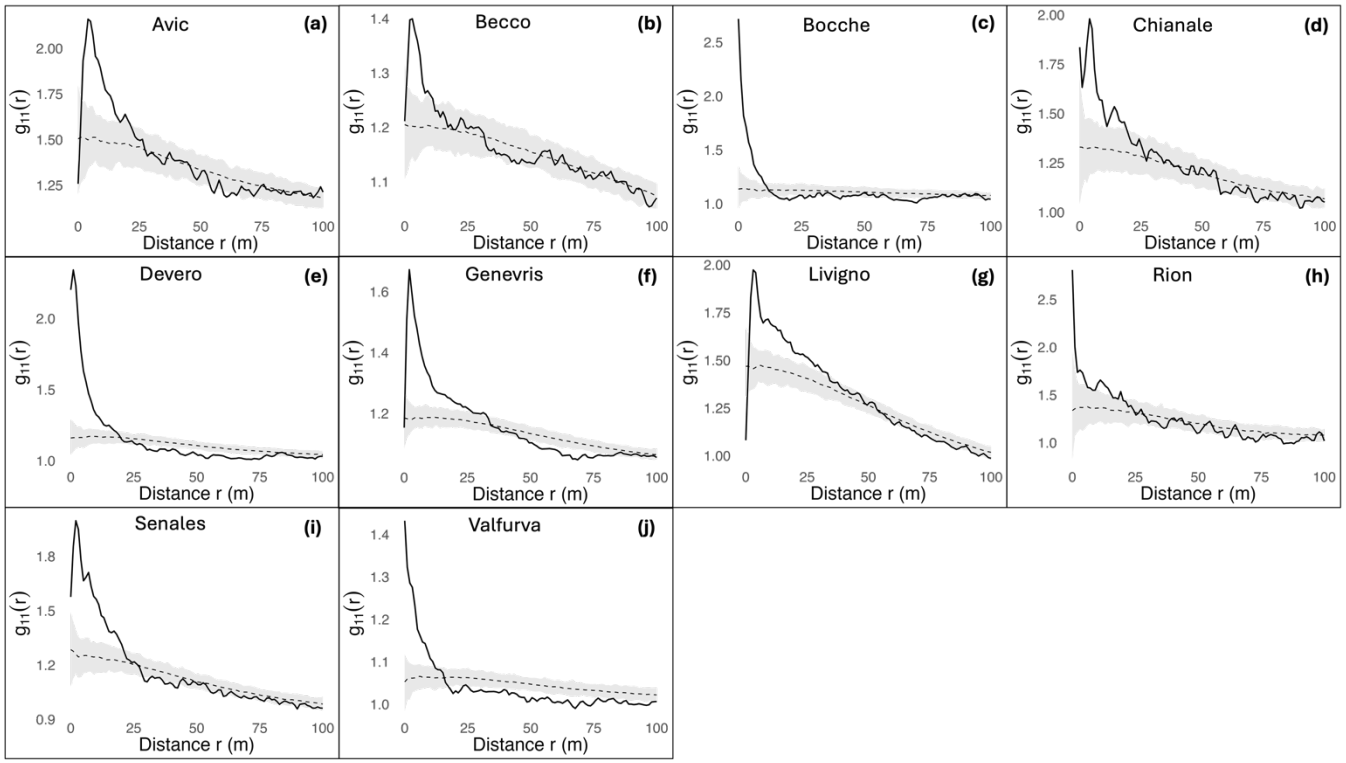

Appendix D:

Figure D1. single sites' results of the bivariate pair-correlation function g12(r) on (a) Avic, (b) Becco, (c) Bocche, (d) Chianale, (e) Devero, (f) Genevris, (g) Livigno, (h) Rion, (i) Senales and (j) Valfurva using point approximation. The confidence envelope (light grey area) represents the upper and lower 95% simulation envelopes. Deviation from the null model (simulation envelope) of the summary statistics (black continue line) indicates a significant attraction (if positive) or repulsion (if negative) between the two patterns.

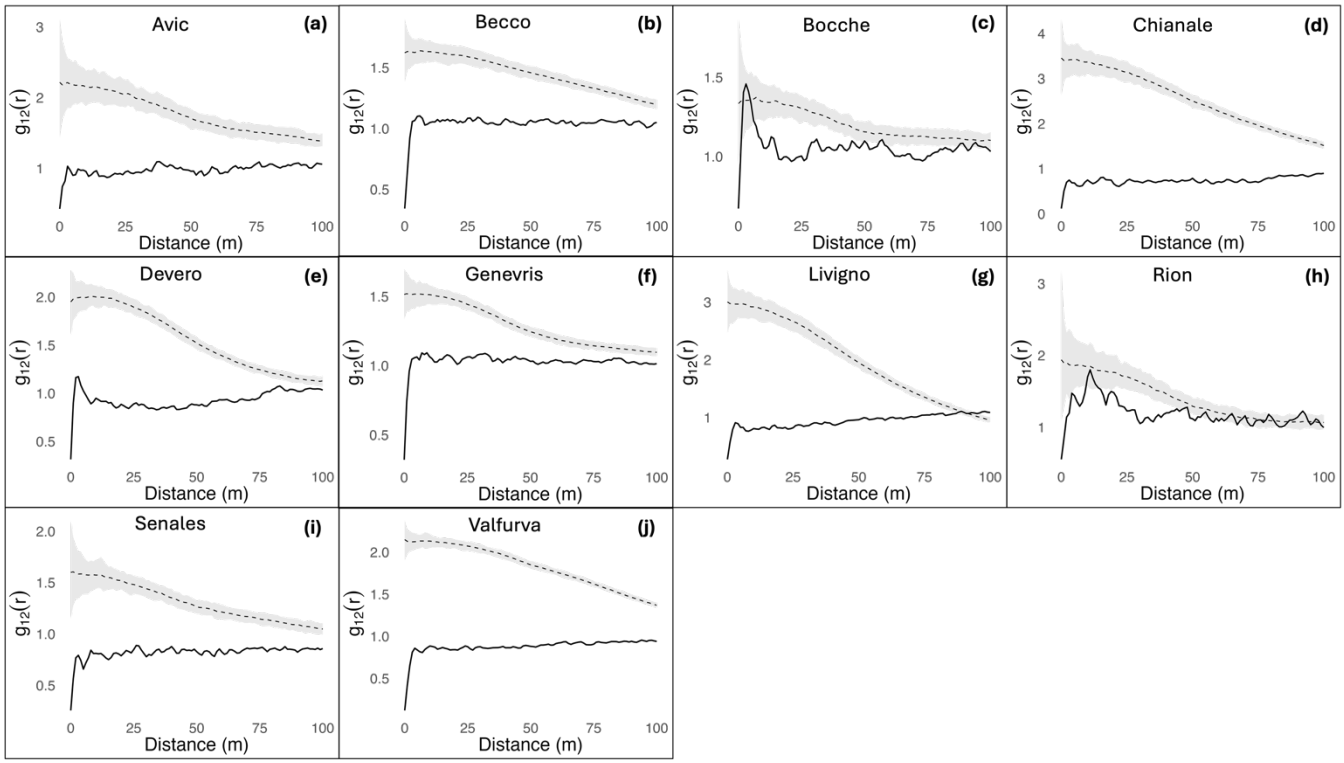

Appendix E:

Figure E1. Univariate pair-correlation function g11(r) for centroids of (a) tall trees, (b) medium trees and (c) small trees. The analysis allows for the definition of a spatial pattern as clumped, random or regular (hyperdispersed) if the summary statistics (black continue line) value is greater than, within, or lower than the confidence envelope (light grey area). The confidence envelope lines represent the upper and lower 95% simulation envelopes. Black dashed lines indicate the expected pattern if the points showed a random spatial distribution.

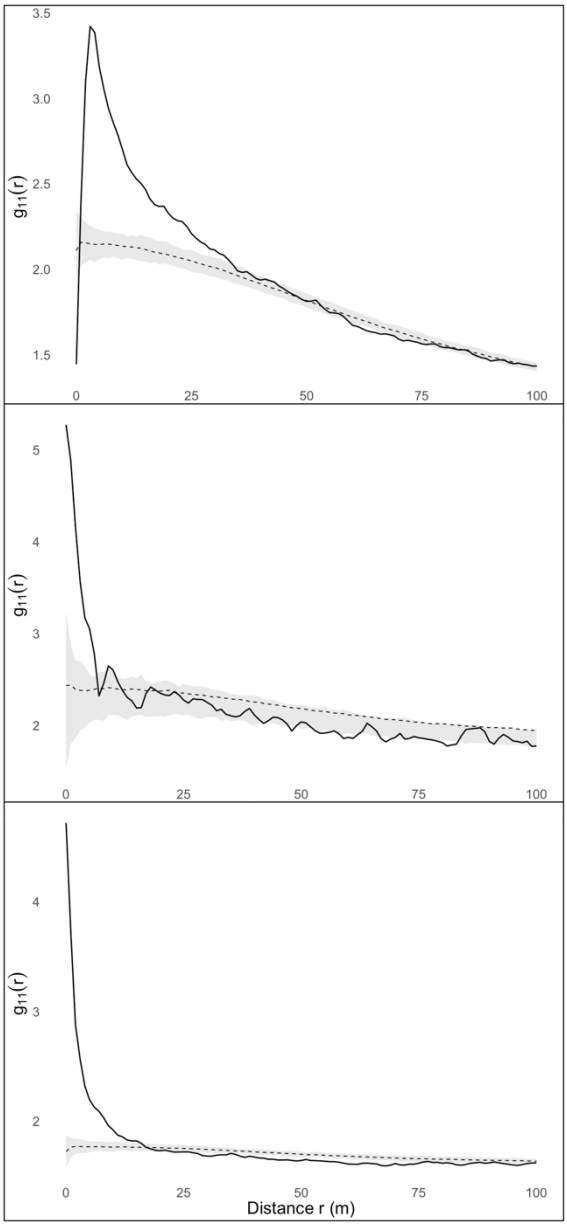

Code availability

The code used in the analysis of this research is available upon request from the first author.

Data availability

The data used in this research are available upon request from the first author.

Author contribution

Carrieri Erik: Methodology, formal analysis, investigation, data curation and writing—original draft preparation. Morresi Donato: Conceptualization, methodology, formal analysis, investigation, data curation, supervision, writing—review and editing. Meloni Fabio: Data collection, data curation, writing—review and editing Anselmetto Nicolò: Conceptualization, methodology, investigation, data curation, supervision, writing—review and editing. Lingua Emanuele: writing—review and editing. Marzano Raffaella: writing—review and editing. Urbinati Carlo: writing—review and editing. Vitali Alessandro: writing—review and editing. Garbarino Matteo: Conceptualization, methodology, investigation, funding acquisition, resources, supervision, writing—review and editing.

Competing interests

The author Garbarino Matteo is Editor of the special issue “Treeline ecotones under global change: linking spatial patterns to ecological processes” to which the paper is submitted.

Special issue statement

This article is part of the special issue "Treeline ecotones under global change: linking spatial patterns to ecological processes”. It is not associated with a conference.

Acknowledgements

This research was funded by the Ministero dell’Università e della Ricerca through the “OLYMPUS - Spatio-temporal analysis of Mediterranean treeline patterns: a multiscale approach” PRIN-2022 project #20225S47P8.

References

Anselmetto, N., Weisberg, P. J., and Garbarino, M.: Global change in the European Alps: A century of post-abandonment natural reforestation at the landscape scale, Landscape and Urban Planning, 243, 104973, https://doi.org/10.1016/j.landurbplan.2023.104973, 2024.

Ball, J. G. C., Hickman, S. H. M., Jackson, T. D., Koay, X. J., Hirst, J., Jay, W., Archer, M., Aubry-Kientz, M., Vincent, G., and Coomes, D. A.: Accurate delineation of individual tree crowns in tropical forests from aerial RGB imagery using Mask R-CNN, Remote Sensing in Ecology and Conservation, 9, 641–655, https://doi.org/10.1002/rse2.332, 2023.

Barros, C., Guéguen, M., Douzet, R., Carboni, M., Boulangeat, I., Zimmermann, N. E., Münkemüller, T., and Thuiller, W.: Extreme climate events counteract the effects of climate and land-use changes in Alpine tree lines, Journal of Applied Ecology, 54, 39–50, https://doi.org/10.1111/1365-2664.12742, 2017.

Bätzing, W., Perlik, M., and Dekleva, M.: Urbanization and Depopulation in the Alps, Mountain Research and Development, 16, 335–350, https://doi.org/10.2307/3673985, 1996.

Beloiu, M. and Beierkuhnlein, C.: Differences in the Spatial Structure of Two Pinus cembra L. Populations in the Carpathian Mountains, Forests, 10, 326, https://doi.org/10.3390/f10040326, 2019.

Beloiu, M., Heinzmann, L., Rehush, N., Gessler, A., and Griess, V. C.: Individual Tree-Crown Detection and Species Identification in Heterogeneous Forests Using Aerial RGB Imagery and Deep Learning, Remote Sensing, 15, 1463, https://doi.org/10.3390/rs15051463, 2023.

Bennett, L., Yu, Z., Wasowski, R., Selland, S., Otway, S., and Boisvert, J.: Individual tree detection and classification from RGB satellite imagery with applications to wildfire fuel mapping and exposure assessments, International Journal of Wildland Fire, 33, https://doi.org/10.1071/WF24008, 2024.

Birre, D., Feuillet, T., Lagalis, R., Milian, J., Alexandre, F., Sheeren, D., Serrano-Notivoli, R., Vignal, M., and Bader, M. Y.: A new method for quantifying treeline-ecotone change based on multiple spatial pattern dimensions, Landsc Ecol, 38, 779–796, https://doi.org/10.1007/s10980-022-01589-4, 2023.

Braga, J. R. G., Peripato, V., Dalagnol, R., Ferreira, M. P., Tarabalka, Y., Aragão, L. E. O. C., de Campos Velho, H. F., Shiguemori, E. H., and Wagner, F. H.: Tree crown delineation algorithm based on a convolutional neural network, Remote Sensing, 12, https://doi.org/10.3390/RS12081288, 2020.

Brieger, F., Herzschuh, U., Pestryakova, L. A., Bookhagen, B., Zakharov, E. S., and Kruse, S.: Advances in the Derivation of Northeast Siberian Forest Metrics Using High-Resolution UAV-Based Photogrammetric Point Clouds, Remote Sensing, 11, 1447, https://doi.org/10.3390/rs11121447, 2019.

Brown, C. D. and Vellend, M.: Non-climatic constraints on upper elevational plant range expansion under climate change, Proceedings of the Royal Society B: Biological Sciences, 281, https://doi.org/10.1098/rspb.2014.1779, 2014.

Cairns, D. M., Lafon, C., Moen, J., and Young, A.: Influences of animal activity on treeline position and pattern: Implications

for treeline responses to climate change, Physical Geography, 28, 419–433, https://doi.org/10.2747/0272-3646.28.5.419, 2007.

Callaway, R. M.: Positive interactions among plants, Bot. Rev, 61, 306–349, https://doi.org/10.1007/BF02912621, 1995.

Callaway, R. M.: Competition and Facilitation on Elevation Gradients in Subalpine Forests of the Northern Rocky Mountains, USA, Oikos, 82, 561–573, https://doi.org/10.2307/3546376, 1998.

Carrer, M., Soraruf, L., and Lingua, E.: Convergent space–time tree regeneration patterns along an elevation gradient at high altitude in the Alps, Forest Ecology and Management, 304, 1–9, https://doi.org/10.1016/j.foreco.2013.04.025, 2013.

Carrer, M., Castagneri, D., Popa, I., Pividori, M., and Lingua, E.: Tree spatial patterns and stand attributes in temperate forests: The importance of plot size, sampling design, and null model, Forest Ecology and Management, 407, 125–134, https://doi.org/10.1016/j.foreco.2017.10.041, 2018.

Castilla, G., Filiatrault, M., McDermid, G. J., and Gartrell, M.: Estimating Individual Conifer Seedling Height Using Drone-Based Image Point Clouds, Forests, 11, 924, https://doi.org/10.3390/f11090924, 2020.

Chan, W.-P., Lenoir, J., Mai, G.-S., Kuo, H.-C., Chen, I.-C., and Shen, S.-F.: Climate velocities and species tracking in global mountain regions, Nature, 629, 114–120, https://doi.org/10.1038/s41586-024-07264-9, 2024.

Coops, N. C., Morsdorf, F., Schaepman, M. E., and Zimmermann, N. E.: Characterization of an alpine tree line using airborne LiDAR data and physiological modeling, Glob Chang Biol, 19, 3808–3821, https://doi.org/10.1111/gcb.12319, 2013.

Crofts, A. L. and Brown, C. D.: The importance of biotic filtering on boreal conifer recruitment at alpine treeline, Ecography, 43, 914–929, https://doi.org/10.1111/ecog.04899, 2020.

Davis, E. L. and Gedalof, Z.: Limited prospects for future alpine treeline advance in the Canadian Rocky Mountains, Global Change Biology, 24, 4489–4504, https://doi.org/10.1111/gcb.14338, 2018.

Dersch, S., Schöttl, A., Krzystek, P., and Heurich, M.: Towards complete tree crown delineation by instance segmentation with Mask R–CNN and DETR using UAV-based multispectral imagery and lidar data, ISPRS Open Journal of Photogrammetry and Remote Sensing, 8, 100037, https://doi.org/10.1016/j.ophoto.2023.100037, 2023.

Dietenberger, S., Mueller, M. M., Bachmann, F., Nestler, M., Ziemer, J., Metz, F., Heidenreich, M. G., Koebsch, F., Hese, S., Dubois, C., and Thiel, C.: Tree Stem Detection and Crown Delineation in a Structurally Diverse Deciduous Forest Combining Leaf-On and Leaf-Off UAV-SfM Data, Remote Sensing, 15, https://doi.org/10.3390/rs15184366, 2023.

Diez, Y., Kentsch, S., Fukuda, M., Caceres, M. L. L., Moritake, K., and Cabezas, M.: Deep learning in forestry using uav-acquired rgb data: A practical review, Remote Sensing, 13, https://doi.org/10.3390/rs13142837, 2021.

Dirnböck, T., Dullinger, S., and Grabherr, G.: A regional impact assessment of climate and land-use change on alpine vegetation, Journal of Biogeography, 30, 401–417, https://doi.org/10.1046/j.1365-2699.2003.00839.x, 2003.

Dirnböck, T., Essl, F., and Rabitsch, W.: Disproportional risk for habitat loss of high-altitude endemic species under climate change, Global Change Biology, 17, 990–996, https://doi.org/10.1111/j.1365-2486.2010.02266.x, 2011.

D'Odorico, P., He, Y., Collins, S., De Wekker, S. F. J., Engel, V., and Fuentes, J. D.: Vegetation–microclimate feedbacks in woodland–grassland ecotones, Global Ecology and Biogeography, 22, 364–379, https://doi.org/10.1111/geb.12000, 2013.

Egli, S. and Höpke, M.: CNN-Based Tree Species Classification Using High Resolution RGB Image Data from Automated UAV Observations, Remote Sensing, 12, 3892, https://doi.org/10.3390/rs12233892, 2020.

Elliott, G. P. and Kipfmueller, K. F.: Multi-scale Influences of Slope Aspect and Spatial Pattern on Ecotonal Dynamics at Upper Treeline in the Southern Rocky Mountains, U.S.A, Arctic, Antarctic, and Alpine Research, 42, 45–56, https://doi.org/10.1657/1938-4246-42.1.45, 2010.

FAO. 1998 FRA 2000 terms and definitions. Forest Resources Assessment Programme working paper 1. FAO, Rome.

Fernández-Guisuraga, J., Sanz-Ablanedo, E., Suárez-Seoane, S., and Calvo, L.: Using Unmanned Aerial Vehicles in Postfire Vegetation Survey Campaigns through Large and Heterogeneous Areas: Opportunities and Challenges, Sensors, 18, 586, https://doi.org/10.3390/s18020586, 2018.

Feuillet, T., Birre, D., Milian, J., Godard, V., Clauzel, C., and Serrano-Notivoli, R.: Spatial dynamics of alpine tree lines under global warming: What explains the mismatch between tree densification and elevational upward shifts at the tree line ecotone?, Journal of Biogeography, 47, 1056–1068, https://doi.org/10.1111/jbi.13779, 2020.

Frei, E. R., Bianchi, E., Bernareggi, G., Bebi, P., Dawes, M. A., Brown, C. D., Trant, A. J., Mamet, S. D., and Rixen, C.: Biotic and abiotic drivers of tree seedling recruitment across an alpine treeline ecotone, Scientific Reports, 8, https://doi.org/10.1038/s41598-018-28808-w, 2018.

Fricker, G. A., Ventura, J. D., Wolf, J. A., North, M. P., Davis, F. W., and Franklin, J.: A convolutional neural network classifier identifies tree species in mixed-conifer forest from hyperspectral imagery, Remote Sensing, 11, https://doi.org/10.3390/rs11192326, 2019.

Fromm, M., Schubert, M., Castilla, G., Linke, J., and McDermid, G.: Automated Detection of Conifer Seedlings in Drone Imagery Using Convolutional Neural Networks, Remote Sensing, 11, 2585, https://doi.org/10.3390/rs11212585, 2019.

Garbarino, M., Malandra, F., Dilts, T., Flake, S., Montalto, L., Spinsante, S., and Weisberg, P. J.: Upper and lower treeline biogeographic patterns in semi-arid pinyon-juniper woodlands, Journal of Biogeography, 47, 2634–2644, https://doi.org/10.1111/jbi.13952, 2020.

Garbarino, M., Morresi, D., Anselmetto, N., and Weisberg, P. J.: Treeline remote sensing: from tracking treeline shifts to multi-dimensional monitoring of ecotonal change, Remote Sensing in Ecology and Conservation, 9, 729–742, https://doi.org/10.1002/rse2.351, 2023.

Gehrig-Fasel, J., Guisan, A., and Zimmermann, N. E.: Tree line shifts in the Swiss Alps: Climate change or land abandonment?, Journal of Vegetation Science, 18, 571–582, https://doi.org/10.1658/1100-9233(2007)18[571:TLSITS]2.0.CO;2, 2007.

Germino, M. J., Smith, W. K., and Resor, A. C.: Conifer seedling distribution and survival in an alpine-treeline ecotone, Plant Ecology, 162, 157–168, https://doi.org/10.1023/A:1020385320738, 2002.

Getzin, S., Dean, C., He, F., A. Trofymow, J., Wiegand, K., and Wiegand, T.: Spatial patterns and competition of tree species in a Douglas-fir chronosequence on Vancouver Island, Ecography, 29, 671–682, https://doi.org/10.1111/j.2006.0906-7590.04675.x, 2006.

Greenwood, S. and Jump, A. S.: Consequences of Treeline Shifts for the Diversity and Function of High Altitude Ecosystems, Arctic, Antarctic, and Alpine Research, 46, 829–840, https://doi.org/10.1657/1938-4246-46.4.829, 2014.

Grimm, V., Revilla, E., Berger, U., Jeltsch, F., Mooij, W. M., Railsback, S. F., Thulke, H.-H., Weiner, J., Wiegand, T., and DeAngelis, D. L.: Pattern-Oriented Modeling of Agent-Based Complex Systems: Lessons from Ecology, Science, 310, 987–991, https://doi.org/10.1126/science.1116681, 2005.

Hamraz, H., Contreras, M. A., and Zhang, J.: Vertical stratification of forest canopy for segmentation of understory trees within small-footprint airborne LiDAR point clouds, ISPRS Journal of Photogrammetry and Remote Sensing, 130, 385–392, https://doi.org/10.1016/j.isprsjprs.2017.07.001, 2017.

Hansson, A., Dargusch, P., and Shulmeister, J.: A review of modern treeline migration, the factors controlling it and the implications for carbon storage, Journal of Mountain Science, 18, 291–306, https://doi.org/10.1007/s11629-020-6221-1, 2021.

Hansson, A., Shulmeister, J., Dargusch, P., and Hill, G.: A review of factors controlling Southern Hemisphere treelines and the implications of climate change on future treeline dynamics, Agricultural and Forest Meteorology, 332, 109375, https://doi.org/10.1016/j.agrformet.2023.109375, 2023.

Hao, Z., Lin, L., Post, C. J., Mikhailova, E. A., Li, M., Chen, Y., Yu, K., and Liu, J.: Automated tree-crown and height detection in a young forest plantation using mask region-based convolutional neural network (Mask R-CNN), ISPRS Journal of Photogrammetry and Remote Sensing, 178, 112–123, https://doi.org/10.1016/j.isprsjprs.2021.06.003, 2021.

Harsch, M. A., Hulme, P. E., McGlone, M. S., and Duncan, R. P.: Are treelines advancing? A global meta-analysis of treeline response to climate warming, Ecology Letters, 12, 1040–1049, https://doi.org/10.1111/j.1461-0248.2009.01355.x, 2009.

Holmgren, P. and Thuresson, T.: Satellite remote sensing for forestry planning—A review, Scandinavian Journal of Forest Research - SCAND J FOREST RES, 13, 90–110, https://doi.org/10.1080/02827589809382966, 1998.

Holtmeier, F.-K. (Ed.): History and Present State of Timberline Research, in: Mountain Timberlines, Springer Netherlands, Dordrecht, 5–10, https://doi.org/10.1007/978-1-4020-9705-8_2, 2009.

Holtmeier, F.-K. and Broll, G.: Treeline advance - driving processes and adverse factors, Landscape Online, 1, 1–33, https://doi.org/10.3097/LO.200701, 2007.

Holtmeier, F.-K. and Broll, G.: Treelines—Approaches at Different Scales, Sustainability, 9, 808, https://doi.org/10.3390/su9050808, 2017.

Holtmeier, F.-K., Broll, G., Müterthies, A., and Anschlag, K.: Regeneration of trees in the treeline ecotone: northern Finnish Lapland, Fennia - International Journal of Geography, 181, 103–128, 2003.

Imangholiloo, M., Saarinen, N., Markelin, L., Rosnell, T., Näsi, R., Hakala, T., Honkavaara, E., Holopainen, M., Hyyppä, J., and Vastaranta, M.: Characterizing seedling stands using leaf-off and leaf-on photogrammetric point clouds and hyperspectral imagery acquired from unmanned aerial vehicle, Forests, 10, https://doi.org/10.3390/f10050415, 2019.

Isotta, F. A., Frei, C., Weilguni, V., Perčec Tadić, M., Lassègues, P., Rudolf, B., Pavan, V., Cacciamani, C., Antolini, G., Ratto, S. M., Munari, M., Micheletti, S., Bonati, V., Lussana, C., Ronchi, C., Panettieri, E., Marigo, G., and Vertačnik, G.: The climate of daily precipitation in the Alps: development and analysis of a high-resolution grid dataset from pan-Alpine rain-gauge data, Intl Journal of Climatology, 34, 1657–1675, https://doi.org/10.1002/joc.3794, 2014.

Jia, M., Zhang, J., Song, Z., and Sadia, S.: Spatial Pattern and Ecological Process Difference Analyses of the Boundary Habitats of a Treeline Patch: A Case Study from the Li Mountain, North China, Land, 11, https://doi.org/10.3390/land11112064, 2022.

Jing, L., Hu, B., Li, J., and Noland, T.: Automated Delineation of Individual Tree Crowns from Lidar Data by Multi-Scale Analysis and Segmentation, Photogrammetric Engineering and Remote Sensing, 78, 1275–1284, https://doi.org/10.14358/PERS.78.11.1275, 2012.

Kattenborn, T., Leitloff, J., Schiefer, F., and Hinz, S.: Review on Convolutional Neural Networks (CNN) in vegetation remote sensing, ISPRS Journal of Photogrammetry and Remote Sensing, 173, 24–49, https://doi.org/10.1016/j.isprsjprs.2020.12.010, 2021.

Körner, C. and Paulsen, J.: A world-wide study of high altitude treeline temperatures, Journal of Biogeography, 31, 713–732, https://doi.org/10.1111/j.1365-2699.2003.01043.x, 2004.

Kyriazopoulos, A., Skre, O., Sarkki, S., Wielgolaski, F., Abraham, E., and Ficko, A.: Human-environment dynamics in European treeline ecosystems: A synthesis based on the DPSIR framework, Climate Research, 73, https://doi.org/10.3354/cr01454, 2017.

Leonelli, G., Masseroli, A., and Pelfini, M.: The influence of topographic variables on treeline trees under different environmental conditions, Physical Geography, 37, 56–72, https://doi.org/10.1080/02723646.2016.1153377, 2016.

Lett, S. and Dorrepaal, E.: Global drivers of tree seedling establishment at alpine treelines in a changing climate, Functional Ecology, 32, 1666–1680, https://doi.org/10.1111/1365-2435.13137, 2018.

Looney, C. E., D'Amato, A. W., Palik, B. J., Fraver, S., and Kastendick, D. N.: Size-growth relationship, tree spatial patterns, and tree-tree competition influence tree growth and stand complexity in a 160-year red pine chronosequence, Forest Ecology and Management, 424, 85–94, https://doi.org/10.1016/j.foreco.2018.04.044, 2018.

Loosmore, N. B. and Ford, E. D.: Statistical Inference Using the G or K Point Pattern Spatial Statistics, Ecology, 87, 1925–1931, https://doi.org/10.1890/0012-9658(2006)87[1925:SIUTGO]2.0.CO;2, 2006.

Mainali, K., Shrestha, B. B., Sharma, R. K., Adhikari, A., Gurarie, E., Singer, M., and Parmesan, C.: Contrasting responses to climate change at Himalayan treelines revealed by population demographics of two dominant species, Ecology and Evolution, 10, 1209–1222, https://doi.org/10.1002/ece3.5968, 2020.

Malandra, F., Vitali, A., Urbinati, C., Weisberg, P. J., and Garbarino, M.: Patterns and drivers of forest landscape change in the Apennines range, Italy, Reg Environ Change, 19, 1973–1985, https://doi.org/10.1007/s10113-019-01531-6, 2019.

Marquis, B., Bergeron, Y., Simard, M., and Tremblay, F.: Disentangling the effect of topography and microtopography on near-ground growing-season frosts at the boreal-temperate forest ecotone (Québec, Canada), New Forests, 52, 1079–1098, https://doi.org/10.1007/s11056-021-09840-7, 2021.

McIntire, E. J. B. and Fajardo, A.: Beyond description: the active and effective way to infer processes from spatial patterns, Ecology, 90, 46–56, https://doi.org/10.1890/07-2096.1, 2009.

Mienna, I. M., Klanderud, K., Næsset, E., Gobakken, T., and Bollandsås, O. M.: Quantifying the roles of climate, herbivory, topography, and vegetation on tree establishment in the treeline ecotone, Ecosphere, 15, https://doi.org/10.1002/ecs2.4845, 2024.

Moir, W. H., Rochelle, S. G., and Schoettle, A. W.: Microscale Patterns of Tree Establishment near Upper Treeline, Snowy Range, Wyoming, U.S.A., Arctic, Antarctic, and Alpine Research, 31, 379–388, https://doi.org/10.1080/15230430.1999.12003322, 1999.

Morley, P. J., Donoghue, D. N. M., Chen, J.-C., and Jump, A. S.: Integrating remote sensing and demography for more efficient and effective assessment of changing mountain forest distribution, Ecological Informatics, 43, 106–115, https://doi.org/10.1016/j.ecoinf.2017.12.002, 2018.

Mottl, O., Flantua, S. G. A., Bhatta, K. P., Felde, V. A., Giesecke, T., Goring, S., Grimm, E. C., Haberle, S., Hooghiemstra, H., Ivory, S., Kuneš, P., Wolters, S., Seddon, A. W. R., and Williams, J. W.: Global acceleration in rates of vegetation change over the past 18,000 years, Science, 372, 860–864, https://doi.org/10.1126/science.abg1685, 2021.

Müller, M., Schickhoff, U., Scholten, T., Drollinger, S., Böhner, J., and Chaudhary, R.: How do soil properties affect alpine treelines? General principles in a global perspective and novel findings from Rolwaling Himal, Nepal, Progress in Physical Geography, 40, 135–160, https://doi.org/10.1177/0309133315615802, 2016.

Næsset, E.: Influence of terrain model smoothing and flight and sensor configurations on detection of small pioneer trees in the boreal-alpine transition zone utilizing height metrics derived from airborne scanning lasers, Remote Sensing of Environment, 113, 2210–2223, https://doi.org/10.1016/j.rse.2009.06.003, 2009.

Næsset, E. and Nelson, R.: Using airborne laser scanning to monitor tree migration in the boreal-alpine transition zone, Remote Sensing of Environment, 110, 357–369, https://doi.org/10.1016/j.rse.2007.03.004, 2007.

Nasiri, V., Darvishsefat, A. A., Arefi, H., Pierrot-Deseilligny, M., Namiranian, M., and Le Bris, A.: Unmanned aerial vehicles (Uav)-based canopy height modeling under leaf-on and leaf-off conditions for determining tree height and crown

diameter (case study: Hyrcanian mixed forest), Canadian Journal of Forest Research, 51, 962–971, https://doi.org/10.1139/cjfr-2020-0125, 2021.

Neuschulz, E. L., Merges, D., Bollmann, K., Gugerli, F., and Böhning-Gaese, K.: Biotic interactions and seed deposition rather than abiotic factors determine recruitment at elevational range limits of an alpine tree, Journal of Ecology, 106, 948–959, https://doi.org/10.1111/1365-2745.12818, 2018.

Nguyen, T.-A., Rußwurm, M., Lenczner, G., and Tuia, D.: Multi-temporal forest monitoring in the Swiss Alps with knowledge-guided deep learning, Remote Sensing of Environment, 305, https://doi.org/10.1016/j.rse.2024.114109, 2024.

Nicoud, B., Bayle, A., Corona, C., Chambard, R. P., Francon, L., Fructus, M., Bensa, M., and Choler, P.: Climate, not land-use, drives a recent acceleration of larch expansion at the forest-grassland ecotone in the southern French alps, Science of The Total Environment, 959, 178326, https://doi.org/10.1016/j.scitotenv.2024.178326, 2025.

Panagiotidis, D., Abdollahnejad, A., Surový, P., and Chiteculo, V.: Determining tree height and crown diameter from high-resolution UAV imagery, International Journal of Remote Sensing, 38, 2392–2410, https://doi.org/10.1080/01431161.2016.1264028, 2017.

Petritan, I. C., Commarmot, B., Hobi, M. L., Petritan, A. M., Bigler, C., Abrudan, I. V., and Rigling, A.: Structural patterns of beech and silver fir suggest stability and resilience of the virgin forest Sinca in the Southern Carpathians, Romania, Forest Ecology and Management, 356, 184–195, https://doi.org/10.1016/j.foreco.2015.07.015, 2015.

Pouliot, D. A., King, D. J., and Pitt, D. G.: Automated assessment of hardwood and shrub competition in regenerating forests using leaf-off airborne imagery, Remote Sensing of Environment, 102, 223–236, https://doi.org/10.1016/j.rse.2006.02.008, 2006.

Qin, H., Zhou, W., Yao, Y., and Wang, W.: Individual tree segmentation and tree species classification in subtropical broadleaf forests using UAV-based LiDAR, hyperspectral, and ultrahigh-resolution RGB data, Remote Sensing of Environment, 280, https://doi.org/10.1016/j.rse.2022.113143, 2022.

Ramírez, L. A., Flinspach, L., Nikolić, N., Toivonen, J., and Bader, M. Y.: Microsite preferences of three conifers in calcareous and siliceous treeline ecotones in the French alps, Alpine Botany, https://doi.org/10.1007/s00035-024-00319-7, 2024.

Rosenberg, M.: Handbook of spatial point-pattern analysis in ecology , by Thorsten Wiegand and Kirk A. Moloney, Boca Raton, FL, Chapman and Hall/CRC, 2013, 538 pp., US$75.00, €78.00, £54.00 (hardback), ISBN 9781420082548, International Journal of Geographical Information Science, 29, 1–2, https://doi.org/10.1080/13658816.2015.1059433, 2015.

Salazar Villegas, M. H., Wiegand, T., González-M, R., Rodriguez-Buritica, S., Qasim, M., and Csaplovics, E.: Spatial facilitation and competition regulate tree species assembly in a tropical dry forest, Front. For. Glob. Change, 6, https://doi.org/10.3389/ffgc.2023.1028515, 2023.

Shimizu, K., Nishizono, T., Kitahara, F., Fukumoto, K., and Saito, H.: Integrating terrestrial laser scanning and unmanned aerial vehicle photogrammetry to estimate individual tree attributes in managed coniferous forests in Japan, International Journal of Applied Earth Observation and Geoinformation, 106, https://doi.org/10.1016/j.jag.2021.102658, 2022.

Simard, M., Pinto, N., Fisher, J. B., and Baccini, A.: Mapping forest canopy height globally with spaceborne lidar, Journal of Geophysical Research: Biogeosciences, 116, https://doi.org/10.1029/2011JG001708, 2011.

Smith, W. K., Germino, M. J., Hancock, T. E., and Johnson, D. M.: Another perspective on altitudinal limits of alpine timberlines†, Tree Physiology, 23, 1101–1112, https://doi.org/10.1093/treephys/23.16.1101, 2003.

Trogisch, S., Liu, X., Rutten, G., Xue, K., Bauhus, J., Brose, U., Bu, W., Cesarz, S., Chesters, D., Connolly, J., Cui, X., Eisenhauer, N., Guo, L., Haider, S., Härdtle, W., Kunz, M., Liu, L., Ma, Z., Neumann, S., Sang, W., Schuldt, A., Tang, Z., van Dam, N. M., von Oheimb, G., Wang, M.-Q., Wang, S., Weinhold, A., Wirth, C., Wubet, T., Xu, X., Yang, B., Zhang, N., Zhu, C.-D., Ma, K., Wang, Y., and Bruelheide, H.: The significance of tree-tree interactions for forest ecosystem functioning, Basic and Applied Ecology, 55, 33–52, https://doi.org/10.1016/j.baae.2021.02.003, 2021.

Vacchiano, G., Castagneri, D., Meloni, F., Lingua, E., and Motta, R.: Point pattern analysis of crown-to-crown interactions in mountain forests, Procedia Environmental Sciences, 7, 269–274, https://doi.org/10.1016/j.proenv.2011.07.047, 2011.

Van Bogaert, R., Haneca, K., Hoogesteger, J., Jonasson, C., Dapper, M., and Callaghan, T.: A century of tree line changes in sub-Arctic Sweden shows local and regional variability and only a minor influence of 20th century climate warming, Journal of Biogeography, 38, 907–921, https://doi.org/10.1111/j.1365-2699.2010.02453.x, 2011.

Vauhkonen, J., Ene, L., Gupta, S., Heinzel, J., Holmgren, J., Pitkanen, J., Solberg, S., Wang, Y., Weinacker, H., Hauglin, K. M., Lien, V., Packalen, P., Gobakken, T., Koch, B., Naesset, E., Tokola, T., and Maltamo, M.: Comparative testing of single-tree detection algorithms under different types of forest, Forestry, 85, 27–40, https://doi.org/10.1093/forestry/cpr051, 2012.

Vitali, A., Camarero, J. J., Garbarino, M., Piermattei, A., and Urbinati, C.: Deconstructing human-shaped treelines: Microsite topography and distance to seed source control Pinus nigra colonization of treeless areas in the Italian Apennines, Forest Ecology and Management, 406, 37–45, https://doi.org/10.1016/j.foreco.2017.10.004, 2017.

Vitali, A., Garbarino, M., Camarero, J. J., Malandra, F., Toromani, E., Spalevic, V., Čurović, M., and Urbinati, C.: Pine recolonization dynamics in Mediterranean human-disturbed treeline ecotones, Forest Ecology and Management, 435, 28–37, https://doi.org/10.1016/j.foreco.2018.12.039, 2019.

Wallace, L., Lucieer, A., Watson, C., and Turner, D.: Development of a UAV-LiDAR system with application to forest inventory, Remote Sensing, 4, 1519–1543, https://doi.org/10.3390/rs4061519, 2012.

Wallace, L., Lucieer, A., Malenovský, Z., Turner, D., and Vopěnka, P.: Assessment of Forest Structure Using Two UAV Techniques: A Comparison of Airborne Laser Scanning and Structure from Motion (SfM) Point Clouds, Forests, 7, 62, https://doi.org/10.3390/f7030062, 2016.

Wang, Y., Mao, Q., Ren, P., and Sigdel, S. R.: Opposite Tree-Tree Interactions Jointly Drive the Natural Fir Treeline Population on the Southeastern Tibetan Plateau, Forests, 12, 1417, https://doi.org/10.3390/f12101417, 2021.

Weinstein, B. G., Marconi, S., Bohlman, S., Zare, A., and White, E.: Individual Tree-Crown Detection in RGB Imagery Using Semi-Supervised Deep Learning Neural Networks, Remote Sensing, 11, 1309, https://doi.org/10.3390/rs11111309, 2019.

Wiegand, T. and A. Moloney, K.: Rings, circles, and null-models for point pattern analysis in ecology, Oikos, 104, 209–229, https://doi.org/10.1111/j.0030-1299.2004.12497.x, 2004.

Wiegand, T., Kissling, W. D., Cipriotti, P. A., and Aguiar, M. R.: Extending point pattern analysis for objects of finite size and irregular shape, Journal of Ecology, 94, 825–837, https://doi.org/10.1111/j.1365-2745.2006.01113.x, 2006.

Williams, A., Allen, C., Macalady, A., Griffin, D., Woodhouse, C., Meko, D., Swetnam, T., Rauscher, S., Seager, R., Grissino-Mayer, H., Dean, J., Cook, E., Gangodagamage, C., Cai, M., and McDowell, N.: Temperature as a potent driver of regional forest drought stress and tree mortality, Nature Climate Change, 3, 292–297, https://doi.org/10.1038/NCLIMATE1693, 2013.

Xiang, B., Wielgosz, M., Kontogianni, T., Peters, T., Puliti, S., Astrup, R., and Schindler, K.: Automated forest inventory: Analysis of high-density airborne LiDAR point clouds with 3D deep learning, Remote Sensing of Environment, 305, https://doi.org/10.1016/j.rse.2024.114078, 2024.

Xie, Y., Wang, Y., Sun, Z., Liang, R., Ding, Z., Wang, B., Huang, S., and Sun, Y.: Instance segmentation and stand-scale forest mapping based on UAV images derived RGB and CHM, Computers and Electronics in Agriculture, 220, https://doi.org/10.1016/j.compag.2024.108878, 2024

Zierl, B. and Bugmann, H.: Sensitivity of carbon cycling in the European Alps to changes of climate and land cover, Climatic Change, 85, 195–212, https://doi.org/10.1007/s10584-006-9201-8, 2007.